

Potential cost savings of large-scale blue hydrogen production via sorption-enhanced steam reforming process

Chinonyelum Udemu, Carolina Font-Palma *

School of Engineering, University of Hull, Hull, HU6 7RX, UK

ARTICLE INFO

Keywords:

Gas-heated reforming
Sorption-enhanced steam reforming
Economic analysis
Hydrogen
CCS

ABSTRACT

As countries work towards achieving net-zero emissions, the need for cleaner fuels has become increasingly urgent. Hydrogen produced from fossil fuels with carbon capture and storage (blue hydrogen) has the potential to play a significant role in the transition to a low-carbon economy. This study examined the technical and economic potential of blue hydrogen produced at 600 MW_{th(LHV)} and scaled up to 1000 MW_{th(LHV)} by benchmarking sorption-enhanced steam reforming process against steam methane reforming (SMR), autothermal gas-heated reforming (ATR-GHR) integrated with carbon capture and storage (CCS), and SMR with CCS. Aspen Plus® was used to develop the process model, which was validated using literature data. Cost sensitivity analyses were also performed on two key indicators: levelised cost of hydrogen and CO₂ avoidance cost by varying natural gas price, electricity price, CO₂ transport and storage cost, and carbon price. Results indicate that, at a carbon price of 83 £/tCO_{2e}, the LCOH for SE-SR of methane is the lowest at 2.85 £/kgH₂, which is 12.58% and 22.55% lower than that of ATR-GHR with CCS and SMR plant with CCS, respectively. The LCOH of ATR-GHR with CCS and SMR plant with CCS was estimated to be 3.26 and 3.68 £/kgH₂, respectively. The CO₂ avoidance cost was also observed to be lowest for SE-SR, followed by ATR-GHR with CCS, then SMR plant with CCS, and was observed to reduce as the plant scaled to 1000 MW_{th(LHV)} for these technologies.

1. Introduction

There has been a strong focus on achieving net-zero emissions, with several initiatives and policies aimed at accelerating the transition to a low-carbon economy. For one, the UK government has outlined measures for achieving net-zero emissions in the 'Ten Point Plan', which includes phasing out the sale of new petrol and diesel cars by 2035, investing in new technologies such as carbon capture and storage (CCS) and increasing the use of renewable energy and low-carbon fuels such as hydrogen [1,2].

Hydrogen has the potential to be a cleaner and sustainable energy carrier, and is produced from a variety of sources, including natural gas, biomass, and renewables. Less than 1 % of hydrogen produced worldwide is generated from renewable sources via electrolysis [3]. Electrolysis splits water molecules into hydrogen and oxygen using electricity from renewable sources [4]. Whilst this method has the advantage of being emission-free, renewable methods of hydrogen production currently face challenges such as low capacity factors due to the intermittent nature of renewable energy sources and higher costs compared to hydrogen produced from fossil fuels. The levelised cost of

green hydrogen varies widely, ranging from 3.84 £/kg to over 8.53 £/kg, depending on the source and cost of electricity used in the hydrogen production process [5,6]. Though this cost is expected to drop in the longer term, fossil fuels are likely to play a role in bridging the gap and complementing renewable energy sources in the medium term, as economies transition to net-zero emissions [7]. Most of the hydrogen today is indeed produced from fossil fuels via processes like gasification and hydrocarbon reforming [8]. In hydrocarbon reforming, feedstocks such as coal, naphtha and natural gas are broken down into hydrogen, carbon monoxide and carbon dioxide via major processes like steam reforming and autothermal reforming [9].

In steam reforming, hydrocarbons are reacted with steam over a catalyst at high temperatures (750 – 1450 °C) and pressure (5–25 atm) [10]. Steam reforming can utilise various hydrocarbons as the feedstock, but the most common application in hydrogen production is steam methane reforming (SMR). In SMR, the main reaction is between methane – typically supplied from natural gas – and steam to produce syngas, under high temperatures of 850–900 °C and elevated pressures of up to 25 bar in the presence of a metal-based catalyst, usually nickel [9]. To increase hydrogen production, the water gas shift reaction is applied after steam reforming to convert the syngas to carbon dioxide

* Corresponding author.

E-mail address: C.Font-Palma@hull.ac.uk (C. Font-Palma).

<https://doi.org/10.1016/j.enconman.2024.118132>

Received 7 August 2023; Received in revised form 1 December 2023; Accepted 21 January 2024

Available online 31 January 2024

0196-8904/© 2024 The Author(s). Published by Elsevier Ltd. This is an open access article under the CC BY-NC-ND license (<http://creativecommons.org/licenses/by-nc-nd/4.0/>).

Nomenclature			
m	Mass flowrate, [kg/s]	PSA	Pressure swing adsorber
n	mole	S/C	Steam-to-carbon ratio
P_e	Electricity consumption, [MWh]	SE-SMR	Sorption-enhanced steam methane reforming
P	Pressure, [bar]	SE-SR	Sorption-enhanced steam reforming
T	Temperature, [°C]	SMR	Steam methane reforming
Abbreviations		TPC	Total plant cost
a-MDEA	Activated methyl diethanolamine	TIC	Total direct installed cost
ATR	Autothermal reforming	Greek	
CCA	Cost of CO ₂ avoided	η	Efficiency, [%]
CCS	Carbon capture and storage	Subscripts	
GHR	Gas-heated reforming	c	Total carbon
LCOH	Levelised cost of hydrogen	e,eff	Electrical efficiency
LHV	Low heating value	NG	Natural gas
		REF	Reference

and hydrogen, in an exothermic reaction. The main process parameters that affect hydrogen yield and energy efficiency in this process are the steam-to-carbon (S/C) ratio, temperature, pressure, and catalyst type. Higher temperatures and pressures favour the forward reaction, while an optimal S/C ratio of 3 is commonly used.

While steam methane reforming is the most prevalent method of hydrogen production today due to its cost-effectiveness, autothermal reforming (ATR) offers some advantages in terms of energy efficiency. In ATR, an oxygen/steam-hydrocarbon mixture is introduced into the reformer at an oxygen-to-carbon and S/C ratios of about 0.6–1 and 0.5–1.5, respectively [11]. An exothermic partial oxidation provides heat for the endothermic steam reforming reactions to proceed [12]. The endothermic reforming of the hydrocarbon produces hydrogen and carbon monoxide. An advanced variation of the traditional SMR, known as gas heated reforming (GHR), can be integrated with an ATR, in a novel configuration. The heat required for steam reforming in the GHR is supplied by heat exchange from a high-temperature effluent gas leaving the ATR, as opposed to furnace used in conventional SMR process [13]. The combined system can serve the purpose of improved energy efficiency (for the SMR side), reduced oxygen consumption and improved H₂/CO ratio (for the ATR side). There are few studies concerning this combined ATR-GHR system available in the public domain [13,14].

Despite the maturity of these reforming technologies, a significant drawback shared by these processes is the generation of carbon dioxide emissions. This has fuelled a growing interest in integrating them with carbon capture technologies, resulting in blue hydrogen production. Amine-based absorption is a widely researched and implemented approach for CO₂ capture from industrial flue gases [15,16] and have been retrofitted into existing reforming plants [17]. Monoethanolamine (MEA) is the most used solvent but its high energy consumption during the regeneration phase is a major concern. This has led to the development of tertiary amines such as methyldiethanolamine (MDEA) as alternative solvents. MDEA, when modified or activated with high CO₂-reactive compounds like piperazine (PZ), enhances CO₂ absorption and reduces energy requirements compared to other amines [18]. Oh et al. [19] evaluated the performance of activated (PZ) MDEA based CCS integrated with hydrogen production plant under different operating parameters such as solvent composition, CO₂ removal efficiency and CO₂ loading. Sensitivity analysis showed CO₂ removal efficiency and solvent composition had great impacts on energy consumption. Optimal PZ and MDEA concentrations varied with CO₂ removal target. At high CO₂ removal efficiency of 95 %, higher MDEA concentration reduced energy needs due to increased solvent flow rate. At 95 % removal efficiency, the reboiler duty slightly decreased when PZ concentration increased from 10 to 15 wt%, whereas at 90 % removal efficiency, the reboiler duty increased for PZ concentrations of 10 % or higher. Similarly, Kum et al.

[20] evaluated the role of activated MDEA solvent to significantly reduce thermal energy requirements and CO₂ capture costs in a medium-sized hydrogen production plant with an output of approximately 5126.5 kmol/h (equivalent to 340 MW_{th} (LHV)). Using process simulation and techno-economic optimisation, they found that at 90 and 99 % CO₂ capture rates, the reboiler duty of the CCS plants was around 70 % lower compared to typical amine-based processes.

Conversely, there are other emerging blue hydrogen technologies under development, including chemical looping reforming, membrane-assisted reforming, sorption-enhanced steam reforming. These technologies aim to increase hydrogen yield and generate pure CO₂ stream that further improves CO₂ capture rates, whilst improving the overall efficiency of the hydrogen production process. Among these emerging technologies, sorption-enhanced steam reforming (SE-SR) has gained particular interest due its compact nature. It combines steam reforming process used to produce hydrogen, with the concept of sorbents capable of selectively adsorbing CO₂. SE-SR works by utilising a sorbent material to adsorb CO₂ in the reforming reactor, which increases the concentration of hydrogen in the product stream. The spent sorbent material is then regenerated by releasing the captured CO₂, which is then purified, compressed and stored separately [21].

Whilst the technology readiness level (TRL) of SE-SR (TRL 6) is currently lower than that of SMR (TRL 9) and ATR-GHR (TRL 9 but relatively new), various parametric studies have demonstrated SE-SR's potential to enhance hydrogen yield and significantly decrease CO₂ emissions. Abbas et al. [22] developed a mathematical model to simulate the performance of SE-SR of methane process under industrially relevant conditions, employing CaO-based sorbent and Ni-based catalyst. The investigation of temperature, pressure, and steam-to-carbon (S/C) ratio revealed that elevated temperatures reaching 650 °C, support reforming reactions and enhances H₂ yield. Higher pressure enhances CO₂ sorption but lowers methane conversion, and a higher S/C ratio improves both methane conversion and H₂ purity, potentially achieving up to 97 %. Similar study had been conducted by Cobden et al. [23] in the past, where they identified the optimal condition for achieving a balance between efficiency, carbon capture, and maintaining the sorbent capacity for SE-SR of methane systems used in power production applications. The set of operating conditions that optimises the performance of the process were found to be at S/C ratio of 4.2, temperature of 600 °C and 17 bar. In fluidised bed reactors, increasing velocities have been found to decrease hydrogen concentration during the SE-SR process. Johnsen et al. [24] conducted a study in a lab-scale bubbling fluidised bed reactor and investigated the effects of increasing velocities, using dolomite as sorbent. They found that as the velocity increased, the hydrogen concentration decreased. However, even at the highest velocity, the hydrogen concentration still exceeded

95 %. Hydrogen yield and efficiency of the SE-SR process is also dependent on the properties of the sorbent used. Ochoa-Fernández et al. [25] evaluated a variety of solid sorbent materials for use in SE-SMR, including K-doped Li_2ZrO_3 , Li_4SiO_4 , Li_2ZrO_3 , CaO and Na_2ZrO_3 . The authors identified CaO and Na_2ZrO_3 as two promising solid acceptor materials for use in SE-SR, with the best efficiencies obtained using CaO due to its high reaction rates. Few studies have also been conducted to examine the economic performance of various configurations of this technology for blue hydrogen production [26–29].

While there have been a few previous studies evaluating the costs of SE-SR for hydrogen production, a direct comparison to other state-of-the-art commercially available options is still lacking in the public domain. Instead, studies were based on economic evaluations of conceptual designs for SE-SR process [26–28]. More recently, Yan et al. [27] explored the economic and technical feasibility of six different sorption-enhanced steam methane reforming (SE-SMR) configurations, at H_2 flowrate of 19.5 t/h, integrated with an indirect natural gas and biomass-fired calciner, chemical-looping combustion and oxy-fuel combustion. The analysis showed that integrating an oxy-fuel combustion calciner can achieve nearly 100 % capture efficiency and lower total capital costs, compared to other technologies within the natural gas feed scenario. They reported a levelised cost of hydrogen ranging from £2.30 to £3.39/kg H_2 (adjusted for inflation).

For a large-scale blue hydrogen production plant, an additional important consideration is hydrogen storage and transmission. Some economic analyses in the literature currently overlook the costs linked to hydrogen storage downstream of production, with initial techno-economic assessments often concentrating solely on the production process. This study lays important groundwork by considering hydrogen storage costs, since hydrogen storage can introduce further capital expenditures and energy penalties that can influence end-user pricing. Several hydrogen storage methods exist, including physical methods like compressed hydrogen, adsorption method, as well as chemical methods such as metal hydrides. However, among these, compressed hydrogen remains the most established storage method [30]. Hydrogen is usually produced at low pressures from these reforming plants; therefore, further compression is required to load the hydrogen into vessels or pipelines for storage and distribution. Centrifugal and reciprocating compressors are generally used for hydrogen compression, with key design factors including the discharge pressure, flow rate and compressor staging [31]. In this work, hydrogen compression to 200 bar is adopted to meet both storage and pipeline transport requirements [32].

SE-SR is a promising hydrogen production technology but remains in its early stages of development, with very few small-scale pilot plants in existence [21]. Because of its low TRL, SE-SR requires further evaluation to strengthen understanding of its real-world costs under scaled-up conditions. Therefore, the aim of this study is to benchmark SE-SR of methane against SMR and ATR-GHR with CCS for large-scale blue hydrogen production, whilst providing insights into the end-to-end potential cost reduction opportunities as the process is scaled up. SE-SR technology and well-established SMR and ATR-GHR processes integrated with piperazine/methyl diethanolamine (a-MDEA) CCS technology were assessed based on a hydrogen production capacity of 600 MW $_{\text{th(LHV)}}$. These processes were also scaled up to 1000 MW $_{\text{th(LHV)}}$ to gain insights into their scalability. To enhance CO_2 removal from high-pressure process gas while reducing reboiler duty, an improved a-MDEA CCS configuration was adopted, which involves splitting and recycling semi-regenerated solvent back into the absorber column. The SE-SR configuration adopted consists of an oxy-fuel combustion unit used to supply heat to the calciner. Cost sensitivity analysis was also conducted for these technologies with the impact of carbon pricing extensively studied. These plants were simulated using Aspen Plus® process simulation software, and the simulation models were validated against literature data.

2. Methods

This study conducts a comparative assessment of SE-SR technology and SMR and ATR-GHR (with CCS) technologies in the context of a newly constructed large-scale hydrogen production facility, including hydrogen compression, in the Humber region, UK. Using natural gas as the major feedstock, 600 MW hydrogen production capacity was evaluated, similar to the proposed capacity for the Hydrogen to Humber (H2H) Saltend project [33]. Methyl diethanolamine blended with an activator – piperazine – (a-MDEA) is used as the CO_2 capture solvent due to its high CO_2 removal rate [18]. SMR without CCS is used as the reference case for performing the cost assessment for the hydrogen plants. These cases are summarised in Table 1.

2.1. Process description and flow diagram

2.1.1. Steam methane reforming (SMR)

The process configuration and conditions for the SMR process studied, follows that of the industrial SMR plant described by Salem et al. [34]. High-pressure natural gas is supplied by the UK National Transmission System (NTS) and laminated to 30 bar. As shown in Fig. 1, the fuel is pre-reformed at 450 °C over a nickel-based catalyst. The pre-reformer unit helps to breakdown the C2-C4 hydrocarbons present in the natural gas, and improve hydrogen yield. Product stream from the pre-reformer is sent to the primary reformer to produce syngas. Due to the highly endothermic nature of steam reforming reaction, the primary reformer is operated at 870 °C and steam-to-carbon ratio of 3, in the presence of a nickel-based catalyst. The generated syngas from the reformer is shifted under medium temperature to produce more hydrogen, which is then sent to the purification section. Using a medium temperature shift converter eliminates the need for two separate shift converters and is operated at a low temperature of 314 °C, in the presence of $\text{CuO}/\text{ZnO}/\text{Al}_2\text{O}_3$ catalyst [35]. The process gas from the shift converter is then directed towards a four-bed pressure swing adsorber (PSA) unit, where 90 % hydrogen is recovered at 99.99 % purity and the PSA off-gas directed to the furnace (with make-up natural gas) to produce heat for the plant [36]. Whilst the heat generated by the furnace is supplied to the reformer, the produced hydrogen is further compressed to a medium pressure of 200 bar to enable transport via pipelines or tube trailers. This SMR process is used as the base case and has no CO_2 capture unit integrated to it, whereas the SMR-CCS cases have CCS unit integrated at the exit of the reformer furnace. The CCS unit is described later in the section.

2.1.2. Sorption-enhanced steam reforming (SE-SR)

The SE-SR process as shown in Fig. 2, includes a dual bubbling fluidised reformer/carbonator and calciner, an oxyfuel combustor, pressure swing adsorption (PSA) columns, heat exchangers and other supporting and auxiliary units. Hydrogen production and CO_2 capture takes place in the same reactor – reformer/carbonator. In the fluidised bed reformer/carbonator, natural gas is reformed with steam at an S/C ratio of 5, in the presence of a nickel-based catalyst to produce mainly hydrogen and CO_2 [37]. The calcined dolomite sorbent material captures the CO_2 generated during the reforming process, thereby shifting

Table 1
Summary of all the cases.

Production capacity	Cases	Description
600 MW	SMR-600	Reference hydrogen production by steam reforming without carbon capture.
	SMR-CCS-600	Hydrogen production by steam reforming with a-MDEA carbon capture.
	SE-600	Sorption-enhanced steam reforming plant
	AG-CCS-600	Autothermal and gas-heated reforming with a-MDEA carbon capture plant.

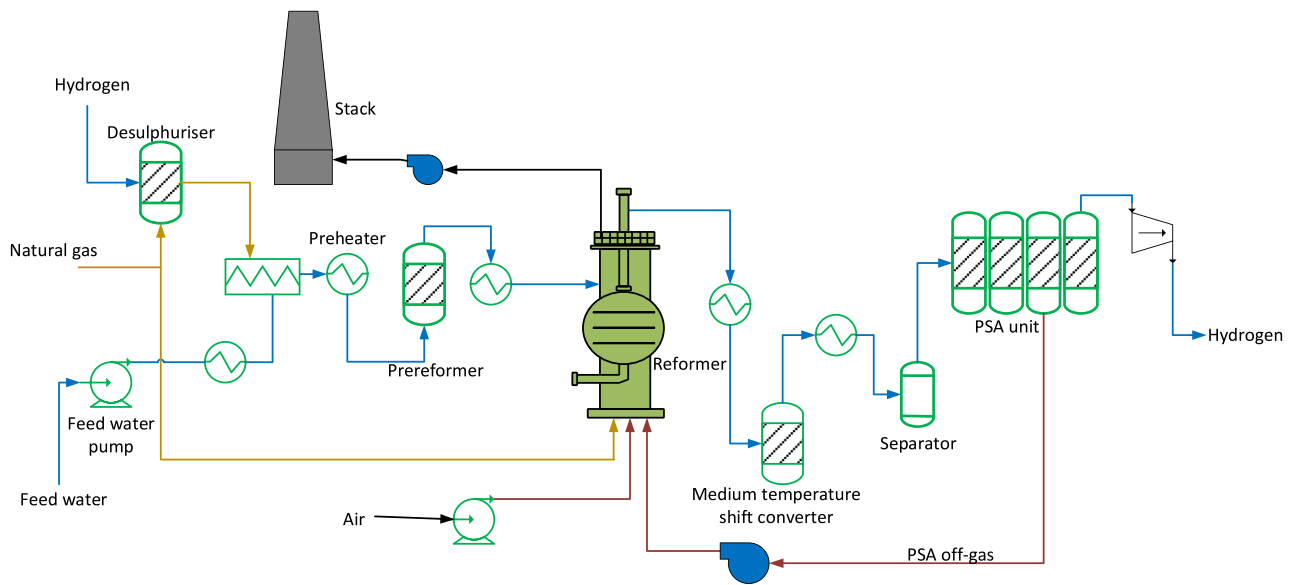


Fig. 1. Process flow diagram for the conventional steam methane reforming process.

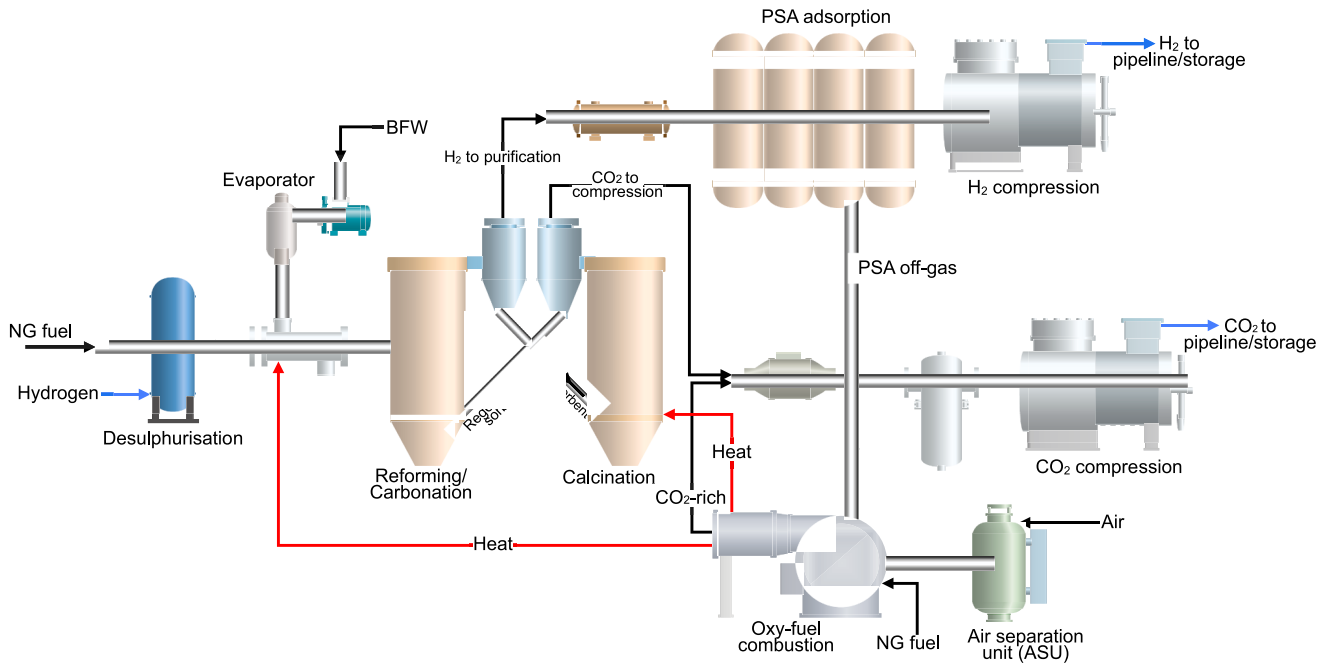


Fig. 2. Process flow diagram for sorption-enhanced steam reforming process.

the equilibrium of the reforming reactions towards higher hydrogen yields, according to Le Chatelier's principle. The spent sorbent is regenerated in the calciner at a high temperature of 900 °C and recycled to the reformer/carbonator [38]. Hydrogen-rich stream from the reformer is sent to the PSA to purify hydrogen to 99.99 % purity with 90 % recovery, and thereafter compressed to 200 bar. The heat required for calcination is supplied by the oxyfuel combustion unit by reacting the PSA off-gas and make-up fuel with pure oxygen provided by the air separation unit (ASU) [39]. Exit stream from the oxyfuel combustion unit is rich in CO₂ and is combined with the CO₂ from the calciner for drying and compression. The CO₂ stream is then compressed to 110 bar for transport.

2.1.3. Autothermal gas-heated reformer with CCS

Fig. 3 presents the hydrogen production process for an autothermal and gas heated reformer with CCS, similar to Johnson Matthey's low carbon hydrogen process [40]. It comprises an autothermal reformer, gas-heated reformer, hydrogen purification and compression unit, a separate carbon capture unit and CO₂ compression unit. Natural gas is first partially reformed in the gas-heated reformer (GHR) at S/C ratio of 1.5 and over nickel-based catalysts, to achieve 30 % methane conversion [41]. The use of the GHR eliminates the need for an external heat source or furnace, as the heat is provided by the hot process gas leaving the ATR. The exit stream of the GHR contains hydrogen, CO₂ and methane at 778 °C and 35.3 bar and is directed to the ATR unit. In the ATR, the feed stream is oxidised with pure oxygen stream from the ASU unit at an oxygen-to-carbon (O/C) ratio of about 1.2, and at high temperature of

solvent alone. In this work, the CO₂ capture unit configuration presented in Fig. 4 is similar to that of BASF carbon capture process, described by Matteo et al. [43]. The CCS unit includes an absorber column, a stripper, low pressure and high-pressure flash drums, as shown in Fig. 4. Information on the column specification and kinetic parameters are contained in the [Supplementary material](#).

For the ATR-GHR plant, the a-MDEA solvent captures CO₂ from the reformer gas stream in the absorber, which is operated at a high pressure of 34 bar similar with the process gas. Operating the absorber at such pressure can improve the CO₂ capture rate. Past studies have been conducted employing high operating pressure for the absorber column [20,44,45]. The CO₂-rich solvent exiting the absorber first enters the high-pressure flash drum operating at 5 bar where some of the reformer gas is recovered, then to the low-pressure flash to regenerate some of the CO₂. Exit stream from the low-pressure flash is split into two; the semi-lean solution recycled back to the absorber and the other stream directed to the stripper at 1.15 bar to completely regenerate the CO₂. The pure CO₂ leaving the CCS unit is compressed to 110 bar for transport. However, for the SMR plant, the CO₂ absorber is operated at a much lower pressure of 6 bar, due to the low pressure of the flue gas leaving the reformer furnace. The configuration of the CCS unit and other components' process conditions remains the same, as described in the previous paragraph. The kinetic parameters and specification of the columns are presented in the [Supplementary material](#).

2.1.5. Hydrogen and CO₂ compression unit

The final state of hydrogen exiting the plant is at a pressure of 200 bar and temperature of 25 °C [32]. A multi-stage centrifugal compressor was employed to achieve four-stage compression, with intercoolers positioned between each stage, as shown in Fig. 5. Flash drums are included to separate any liquids present and an equal pressure ratio is applied between each stage. The hydrogen feed at from the hydrogen purification unit enters Compressor 1, where it is compressed. Upon exiting, the hot compressed gas flows through an intercooler where cooling water lowers its temperature to 30 °C. Now at an elevated pressure, it enters Compressor 2 for further compression. Again,

intercooling cools the gas before the Compressor 3 further pressurises it. A final intercooler prepares the gas for the fourth stage compressor. From here, the hydrogen gas passes through a final cooler to reduce the temperature to 25 °C. More information on the operating conditions and parameters is presented in [Table 3](#).

2.2. Process simulation

A commercial simulation tool, Aspen Plus®, was used to evaluate the mass and energy for the processes studied. Peng-Robinson-Boston-Mathias (PR-BM) and Steam-National Bureau of Standards (Steam-NBS) equation of state (EOS) was used for SMR, SE-SR and ATR-GHR hydrogen production section of the plant, while the Electrolyte NRTL model was used for the a-MDEA CO₂ capture process. The PR-BM EOS is suitable for modelling hydrocarbon systems, including natural gas and hydrogen, at high pressures [46]. Steady-state conditions were assumed for all the processes, with uniform temperatures and pressures in the reforming reactors. The reactions used to model the processes, including the CO₂-PZ-MDEA system are presented in the [Supplementary material](#). The main model inputs and operating conditions are presented in [Table 2](#) and [Table 3](#). All process flowsheets developed in Aspen Plus are shown in the [Supplementary material](#).

Table 2
Natural gas composition [47].

Components	Values (%mol)
CO ₂	0.780
CH ₄	92.420
N ₂	2.880
Ethane	0.302
Propane	0.590
C ₄ +	0.310

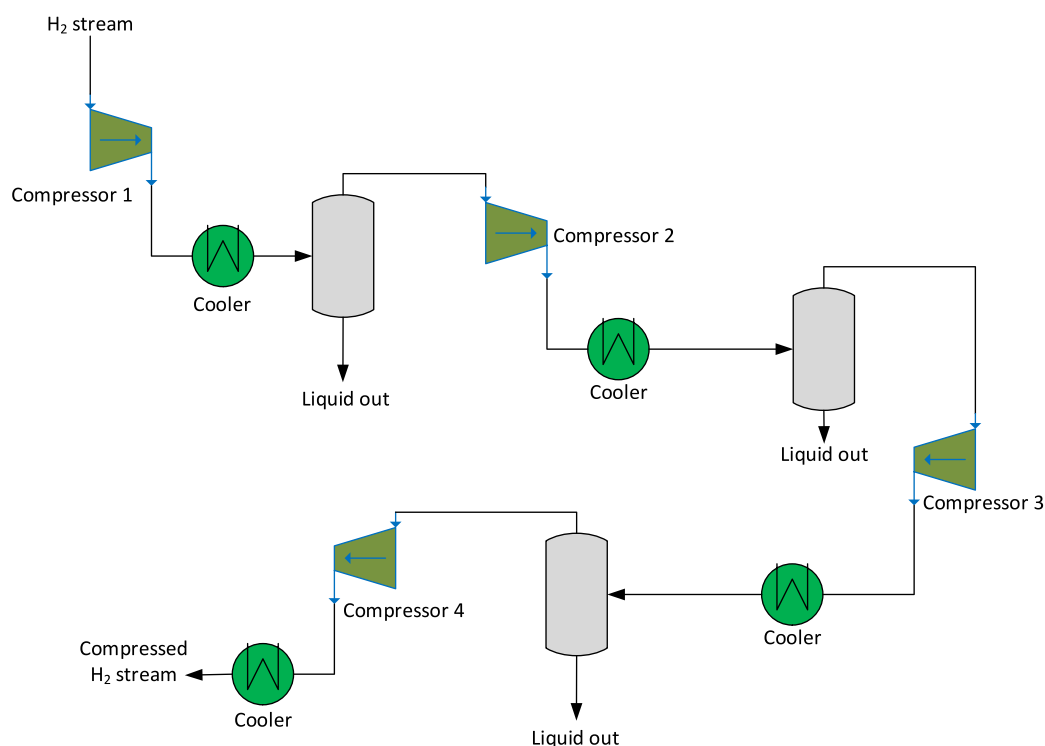


Fig. 5. Process flow diagram of the hydrogen compression system.

Table 3
Operating conditions and key units used in the model.

Process units	Aspen unit model	Parameter	Value	Unit	Ref
Reformer/ carbonator	RGibbs	Temperature	600	°C	[48]
Calciner	RGibbs	Temperature	900	°C	[48]
		Pressure	1	Bar	[48]
ATR	RGibbs	Temperature	1050	°C	[11]
Medium temperature shift converter	RStoic	Temperature	270—313	°C	[34]
Pumps	Pump	Mechanical Efficiency	85	%	[49]
Oxy-fuel combustor	RStoic	Pressure	5	Bar	[50]
		Oxygen purity	99	%	[51]
H ₂ compressor	MCompr	Isetropic efficiency	60	%	[52]
		Mechanical efficiency	92	%	[52]
		Intercooling temperature	30	°C	[53]
		Final stage H ₂ cooler	25	°C	[53]
CO ₂ compressor	MCompr	Isetropic efficiency	80	%	[54]
		Mechanical efficiency	97	%	[54]
		Number of compression stages	4	–	[54]
		Intercooling temperature	30	°C	[55]
		Final stage CO ₂ cooler	30	°C	[55]
		temperature			

2.3. Process performance indicators

The performance of each of the processes were analysed using some key performance indicators including net process efficiency, cold gas efficiency, carbon capture efficiency, specific CO₂ emissions and specific CO₂ captured. The equations for calculating these parameters are presented in Table 4. Natural gas to electrical conversion efficiency, $\eta_{e,eff}$ of 49 % was used, which corresponds to the average thermal efficiency of combined cycle gas power stations in the UK [56].

2.4. Economic assessment

The IEAGHG cost method and criteria for CCS plants and plants with low CO₂ emissions was used to estimate elements of the capital and operating costs for each of the hydrogen plants and is presented in Table 5 [57,58]. Total Direct Cost (TDC) includes the direct costs of all

Table 4
Technical performance indicators for the processes.

Parameters	Equations	No
Methane conversion (%)	$\left(1 - \frac{n_{CH_4,out}}{n_{CH_4,in}}\right) \times 100\%$	1
Cold Gas Efficiency (%)	$\frac{m_{H_2} \times LHV_{H_2}}{m_{NG,total} \times LHV_{NG}}$	2
Net Process Efficiency (%)	$\left(\frac{m_{H_2} \times LHV_{H_2}}{m_{NG,total} \times LHV_{NG}} + \frac{P_e}{\eta_{e,eff}}\right) \times 100\%$	3
Overall Carbon Capture efficiency (%)	$\left(\frac{n_{CO_2,compressor}}{n_{CO_2,total}}\right) \times 100\%$	4
Specific CO ₂ Emissions (kg _{CO₂} /kg _{H₂})	$\frac{m_{CO_2}}{m_{H_2} \times LHV_{H_2}}$	5

Table 5
Economic criteria applied to each of the plants (TDC = Total direct cost; TPC = Total plant cost) [57,58].

Parameters	Values	Ref
Plant life	25 Years	
Capacity factor: Year 1, Year 2 – 25	70 %, 95 %	
EPC	30 % TDC	
Construction	20 % TDC	
Other costs	0.5 % TDC	
Contingency	20 %TPC (40 % for SE-SR)	
Working capital	Inventories for chemicals and materials for extra one month	
Spare parts cost	0.5 % TPC	
Owner's costs	7 % TPC	
Annual operating and maintenance cost	2.1 % TPC	
Administrative and general overhead cost	30 % of direct and maintenance labour cost	
Indicative costs	2.5 % TPC	
Insurance	0.5 % TPC	
Local taxes and fees	0.5 % TPC	
Construction period	3 Years	
Capital Expenditure Curve		
Year 1	25 %	
Year 2	45 %	
Year 3	30 %	
Discount rate (Initial)	8 %	
Variable costs		Ref
Electricity, (£/MWh)	135.60	[62,63]
Natural gas, (£/GJ)	12.75	[63,64]
Water, (£/m ³)	0.8517	[65]
Catalysts, (£/ton)	11,704	[66]
MDEA, (£/ton)	2,400	[67]
Piperazine, (£/ton)	22,399	[68]
Dolomite, (£/ton)	80	[69]
CO ₂ transport & storage (offshore), £/tCO ₂ stored	10	[70]
Carbon price, (£/tCO _{2e})	83.03	[71]

equipment required for the plant as well as direct project costs like installation. The total plant cost (TPC) was calculated from the sum of all the costs captured in TDC, EPC services, contingencies, and upon addition of owner's cost, results in the total capital requirement (TCR) for the various blue hydrogen plants. Conversely, the operating and maintenance labour, overheads, property taxes, insurance, fuel, electricity and other consumables were considered in the estimation of the operating cost, with all the cost projections' level of accuracy categorised under the AACE Class 4. A contingency of 40 % was applied to the SE-SR plants due to its low maturity level. A comprehensive equipment cost scaling approach based on the correlation by Peters et al. [59] was employed for the main reactors including the ATR, GHR, reformer/carbonator, calciner, considering the Chemical Engineering Plant Cost Index (CEPCI) and accounting for the impact of inflation over time. Details of the parameters used in estimating the equipment cost is reported in the Supplementary material. The January 2023 CEPCI was used for the calculations, while the March 2023 Oanda exchange rate was used to convert Euros and USD to Pound sterling, £ [60]. Installed costs of the remaining plant components were obtained from Aspen Process Economic Analyser® (APEA), using the 2019 UK currency basis. The levelised cost of hydrogen (LCOH) was evaluated by dividing the net present value of the total hydrogen production cost by the net present value (NPV) of hydrogen produced over the plant's lifetime, as published by the Department for Energy Security and Net Zero, DESNZ (formerly Department for Business, Energy & Industrial Strategy, BEIS) [61].

$$NPV \text{ of Total costs} = \sum_n \frac{\text{Total CAPEX and OPEX}_n}{(1 + \text{discount rate})^n} \quad 6$$

$$NPV \text{ of hydrogen production} = \sum_n \frac{\text{Hydrogen production}_n}{(1 + \text{discount rate})^n} \quad 7$$

$$\text{Levelised Cost of Hydrogen} = \frac{\text{NPV of total costs}}{\text{NPV of hydrogen production}} \quad 8$$

where n is the period. The cost of CO₂ avoidance is calculated from equation (9).

$$\text{Cost of CO}_2 \text{ avoided (CCA)} = \frac{\text{LCOH}_{\text{CCS}} - \text{LCOH}_{\text{REF}}}{\text{CO}_2\text{Emissions}_{\text{REF}} - \text{CO}_2\text{Emissions}_{\text{CCS}}} \quad 9$$

2.4.1. Estimation of CO₂ emissions cost

Carbon pricing mechanisms effectively quantify the cost of CO₂ emissions, making it a crucial factor in evaluating the economic viability of hydrogen production from fossil fuels. In recent years, the UK has focused on two primary carbon pricing mechanisms to reduce emissions – the EU Emissions Trading System (EU ETS) and the UK Carbon Price Support (CPS) mechanism [72]. However, following Brexit, the UK replaced the EU ETS with its independent Emissions Trading Scheme (UK ETS), which continues to operate on the same cap-and-trade principles but with a separate market for allowances.

Given the uncertain long-term prospects of the CPS policy and its focus on the use of fossil fuels for power generation, the carbon price used in this study is based on only the UK ETS pricing, to ensure a consistent carbon price signal throughout the hydrogen plant's lifetime. Therefore, a carbon price of £83.03/tCO₂e set by the UK ETS for January 1, 2023, is applied in this study [71].

2.4.2. Estimation of hydrogen compressor cost

Hydrogen compression would be required for most production technologies, if the hydrogen needs to be stored or transported via pipelines to end-users [61]. Therefore, this analysis assumed that hydrogen will be compressed to 200 bar to accommodate both storage and pipeline transportation [73,74]. The installed cost of hydrogen compressor was calculated based on the correlations by Khan et al. [75], which depends on the power requirements of the compressor motor.

$$\text{Total installed cost, CAD\$} = 2 \times (3083.3 * kW^{SF}) \quad 10$$

Where Scale factor, SF = 0.8335 and kW is the compressor power. The installed cost is escalated from 2019 to 2023 rate using the Chemical Engineering Plant Cost Index (CEPCI) and converted to £.

2.4.3. Sensitivity analysis

Sensitivity analysis was conducted to determine the impact of ± 50 % variations in key parameters such as natural gas prices, electricity prices, CO₂ emissions costs and discount rate on the LCOH and CCA. Using the operating cost assumptions in Table 5 as the baseline values, the sensitivity ranges are presented in Table 6.

3. Results and discussion

In this section, we present the key findings from the process simulation and economic evaluation of the hydrogen production processes. The simulation was carried out using Aspen Plus software to model material and energy balances across the system. Detailed material and stream tables for the flowsheet are provided in the [Supplementary Material](#).

Table 6
Sensitivity ranges used for the cases.

Sensitivity variables	Units	Lower bound	Baseline	Upper bound
Feedstock and fuel price	£/GJ (LHV)	9.38	12.75	19.13
Electricity price	£/MWh	101.7	135.60	203.4
Discount rate	%	6	8	12
CO ₂ transport & storage (offshore)	£/tCO ₂ stored	7.5	10	15
CO ₂ emission costs	£/tCO ₂ e	62.25	83	124.5

3.1. Model validation

In this section, the validation results of the simulated plants in Aspen Plus and the comparison with experimental data obtained from relevant literature are presented. Model validation was conducted and relative errors, although small, are reported with the understanding that the subsequent results may have a small error. To validate the simulation results, the operating conditions from the literature were replicated in the simulations. Subsequently, the simulation outcomes were compared to the experimental findings. For the SMR and SE-SR processes, the comparison was conducted based on the composition of the product streams from the main reactors in the processes. In the ATR-GHR plant, the comparison was based on the energy input required for the overall process.

The simulated SE-SR plant was validated with experimental data from Martínez et al. [48]. By comparing the reformer outlet compositions obtained from the SE-SR process model with experimental data, a good agreement was observed at the outlet composition, as shown in Fig. 6, except for Fig. 6b which showed a slight deviation for methane composition at temperatures between 600 and 700 °C. In addition, the model slightly overestimated CH₄ conversion and H₂ yield, as presented in the [supplementary material](#). However, the absolute errors between the simulation and literature data were calculated to be less than 14 % and 2 % for H₂ yield and CH₄ conversion, respectively. This deviation is caused by the difficulty in balancing the temperature approaches for the steam reforming reaction and carbonation reaction. Nevertheless, the range of relative error indicates an acceptable level of accuracy for the developed model [76,77].

The validation of the simulated SMR plant utilised data from a ~ 60MWth_(LHV) SMR plant reported by Salem et al. [34], while that of the ATR-GHR plant relied on output data reported by Johnson Matthey for a 322 MWth_(LHV) hydrogen production capacity [40]. The results for the SMR process were consistent with the reported values as seen in Fig. 7. For an ATR-GHR-CCS plant with hydrogen production capacity of 107.4 kNm³/hr, the required natural gas feed obtained from literature is 38.31 kNm³/hr [40], compared to our simulated plant requiring 39.108 kNm³/hr. The relative error between literature data and our simulated result is 2 %, which is acceptable for this study's objectives and the level of accuracy typically achievable in process simulations [34]. Therefore, the model was used for further simulations. (Fig. 7).

It should be acknowledged that while the validation studies in this work have provided favourable results, availability of data beyond bench-scale conditions could further enhance the robustness and applicability of the developed model, especially for the SE-SR plant.

3.2. Energy requirements

In modelling the hydrogen production plants, a power island was included to account for the on-site electricity demand. The power island consists of a steam turbine sized to meet the average steam flow supplied by the heat recovery steam generator (HRSG). Waste heat from each of the hydrogen production processes is used to generate high pressure steam in the HRSG.

The main source of energy in the plants is natural gas, which is also used as the feedstock. The total natural gas required for each of the plants is presented in Fig. 8. A relatively high fuel input is seen in the SMR-CCS-600 plant, where it consumes 0.4 % – 16 % more natural gas than the other plants, due to the extra fuel used to provide energy for auxiliary components like compressors and generating steam for the CCS plant. The integration of an a-MDEA CCS unit into the SMR plant for blue hydrogen production resulted in an 18 % increase in overall fuel consumption. This increase is relatively lower compared to the findings of Oni et al. [72], who reported a higher fuel consumption penalty (39 %) for an SMR plant integrated with a MEA CCS system, for a slightly higher hydrogen production capacity (about 760 MWth_(LHV)). Despite having a slightly higher hydrogen production capacity than our SMR-CCS-600

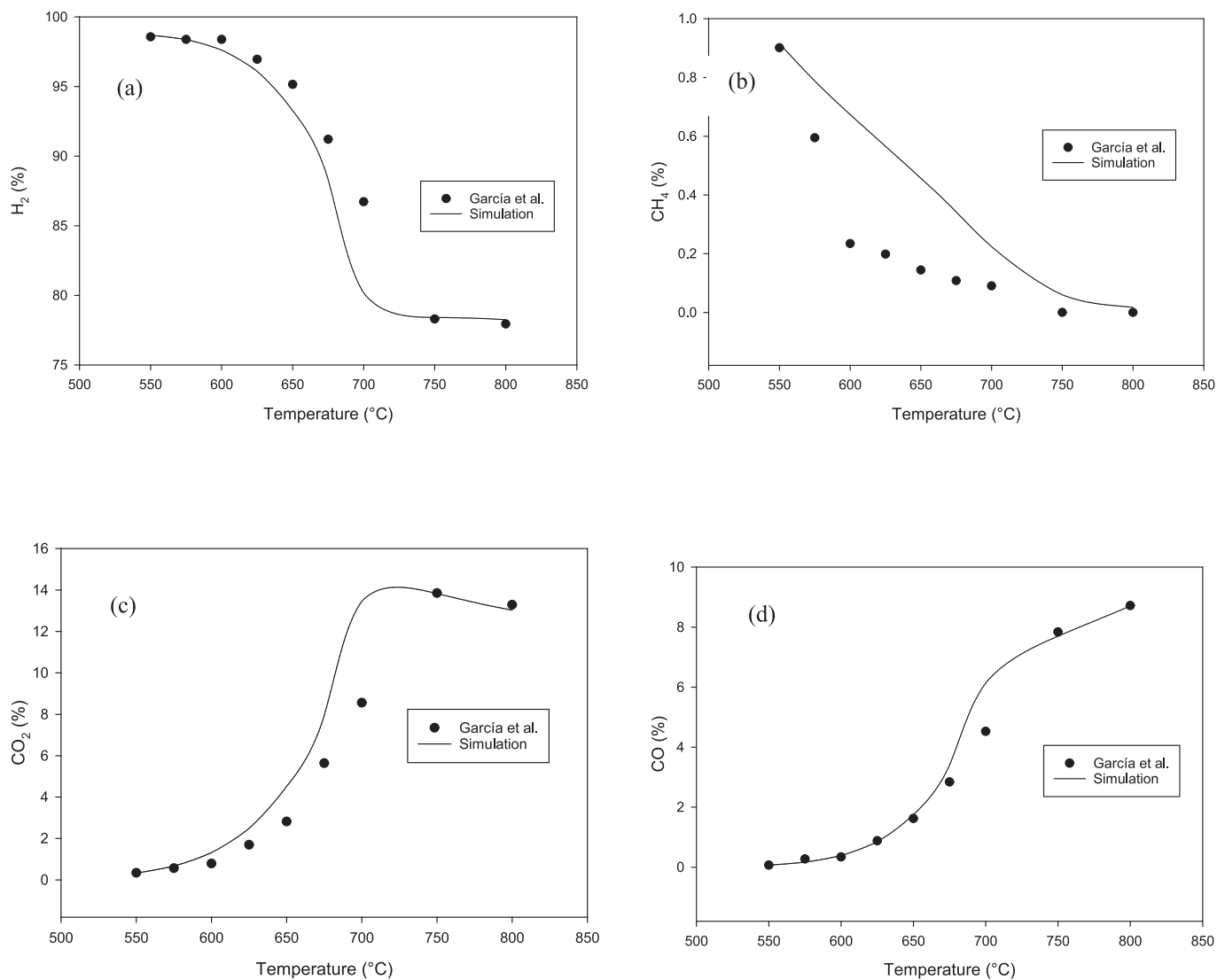


Fig. 6. Comparison of gas compositions (on dry basis) between experimental [48] and simulated data for SE-SR of methane at different reactor temperatures.

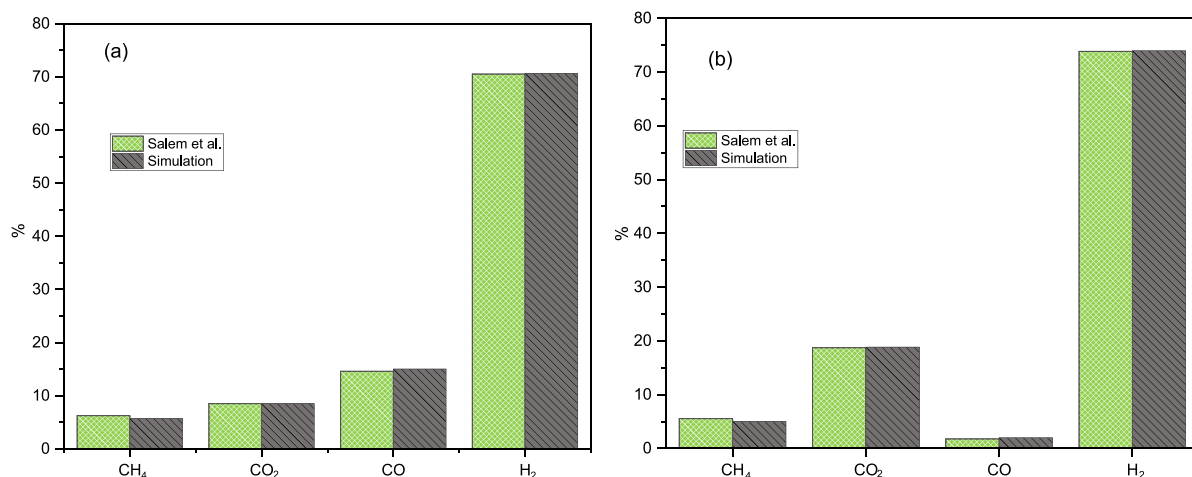


Fig. 7. Outlet compositions from (a) the reformer and (b) the shift converter, contrasting plant data [34] with simulation results for the SMR process.

system, our scaled-up 1000 MWth plant still exhibited a 16 % increase in fuel consumption compared to the baseline SMR plant, for a similar CO₂ capture efficiency. Studies have indicated that employing a-MDEA

solvent leads to a reduction in overall CCS energy consumption, largely attributed to a decline in reboiler energy requirements compared to other amine solvents [42,45].

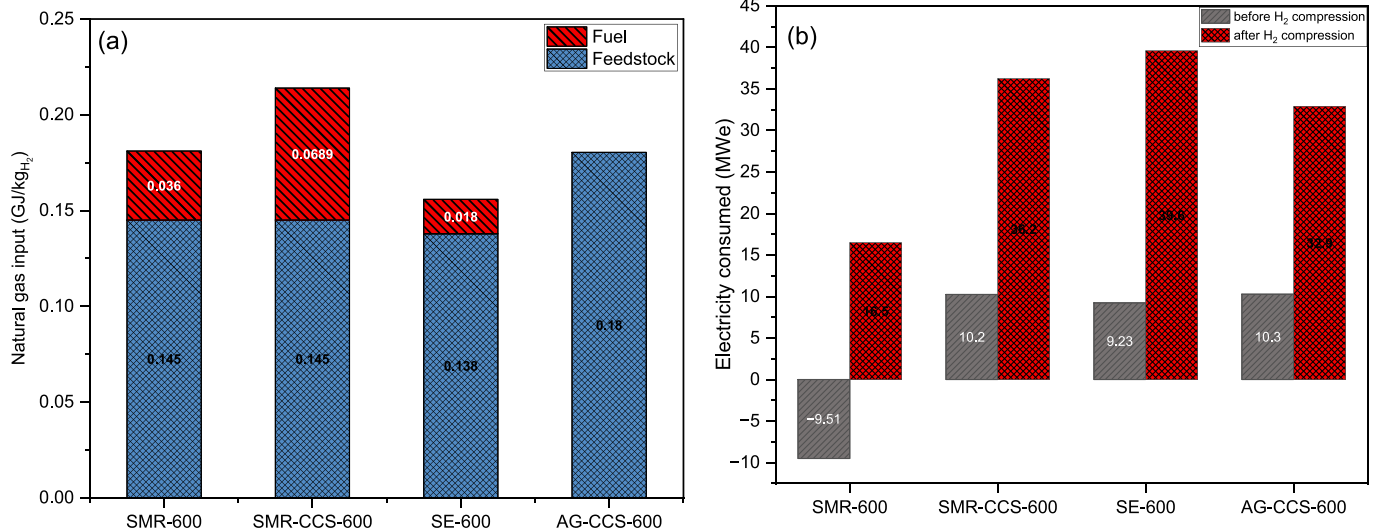


Fig. 8. (a) Natural gas and (b) Electrical requirement for the hydrogen production plants.

The fuel consumption of AG-CCS-600 is slightly lower than that of SMR-CCS-600 by 0.4 %, which could be attributed to different reasons: the gas heated reformer design in AG-CCS-600 allows for effective heat recovery, which maximises energy recycling and drives the endothermic reforming reactions with less external fuel input. Fuel consumption in SE-600 is observed to be the lowest, at 13 % – 27 % lower than the rest of the hydrogen plants. Apart from having fewer process units which means the carbon capture system imposes a smaller energy penalty on the plant, the thermally neutral nature of the process must have played a role. In SE-SR, the heat energy required for steam reforming reaction is provided by the exothermic carbonation reaction, resulting in less heat input [21]. Fig. 8a compares the energy requirements of the various hydrogen production technologies. It shows the amount of natural gas (NG) input required to produce one kilogram of hydrogen for each method. SE-600 has the lowest total NG requirement at around 0.156 GJ/kgH₂, whereas AG-CCS-600 requires more energy input at around 0.18 GJ/kgH₂. SMR-CCS-600 has the highest NG demand, necessitating about 0.21 GJ of input to generate 1 kg of hydrogen.

Electricity produced was insufficient to fully meet the plant's electrical needs. Therefore, the final integrated process-power system model also included the ability to import additional electricity from the local grid network. Fig. 8b reveals the electricity consumption of the various hydrogen production technologies and how much additional power is needed to compress the produced hydrogen gas for storage and transport.

Before hydrogen compression, AG-CCS-600 required the most power at around 10 MWe, followed by SMR-CCS-600 at about 10.2 MWe and SE-600 at 9.23 MWe. SMR-600 plant has an electricity excess of 9.51 MWe, which can be exported. The substantial electricity consumption of SMR-CCS-600 stems from the operation of air and PSA off-gas compressors (with large flowrates of air and off-gas), which are essential for the reformer furnace to provide thermal energy for the process. In the process design, reformer gas from the shift converter was purified, and PSA off-gas was routed back to the reformer furnace below 1 bar, thereby requiring compression for use as fuel. This configuration was adopted to capture CO₂ from the reforming furnace flue gas. CO₂ capture from furnace flue gas is recognised as the most efficient approach, as it yields the most concentrated CO₂ stream from steam reforming plant [78]. Additionally, the high natural gas input meant increased volume of CO₂ generated, consequently requiring more compression power downstream.

When hydrogen compression is included, the relative differences change significantly. This is due to differences in the initial hydrogen

pressure before compression between technologies. SE-600 tops the list, requiring an additional electricity import of 30.6 MWe. SE-600 operates at relatively low pressure compared to SMR-CCS-600 and AG-CCS-600, so high compression ratio is required to compress H₂ to 200 bar. Despite the equilibrium benefits offered by the sorbent, lower pressure conditions continue to favour the thermodynamics of the underlying steam reforming reaction [79]. SMR-CCS-600 also saw a sharp rise by 26 MWe due to its compression load. In contrast, AG-CCS-600 experienced a relatively low increase by 22.60 MWe.

Hydrogen compression is a significant contributor to the power demand of SMR-CCS-600, SE-600, and AG-CCS-600 plants. It accounts for 71.74 %, 76.70 %, and 68.76 % of the total power demand in these plants, respectively. This high demand for power entails additional electricity imports, which increase by 254 %, 329 %, and 220 %, respectively, for these plants.

3.3. Net process efficiency

A key performance metric for any production process is its overall energetic efficiency. Fig. 9a illustrates the cold gas efficiencies achieved by the different hydrogen plants. SE-600 performed best with a cold gas efficiency of 82.82 %, attributed to the thermally neutral characteristics of the process. SMR-600, SMR-CCS-600 and AG-CCS-600 realised cold gas efficiencies around 71.25 %, 60.30 % and 72 %, respectively.

Fig. 9b displays the process efficiencies achieved through simulations of different blue hydrogen production pathways. In this study, the power requirement for the auxiliary components, including the ASU, compressors and PSA, was considered in the calculation of the net process efficiency. Before H₂ compression, SE-600 achieved the highest net efficiency of around 79.6 %, followed closely by AG-CCS-600 at 70.14 %, then SMR-CCS-600 at a lower net efficiency of 60 % due to its demand for external fuel. Its lower net efficiency, compared with SMR-600 also indicates greater energy penalty associated with downstream CO₂ capture and compression. Conversely, the AG-CCS-600 improved process efficiency compared to SMR-CCS-600 was primarily due to the reduced energy inputs and power needs in the AG-CCS design, which lessened the efficiency penalties associated with the CCS. Integrating hydrogen compression to each of the plants saw a reduction in the net process efficiency of all the plants. SE-600 maintained the highest net process efficiency, while AG-CCS-600 achieved a higher net process efficiency of around 66.56 % than SMR-600 at 56.12 %. SMR-CCS, SE-600 and AG-CCS net efficiencies still decreased by 3–5 percentage points when hydrogen compression was added versus their non-H₂

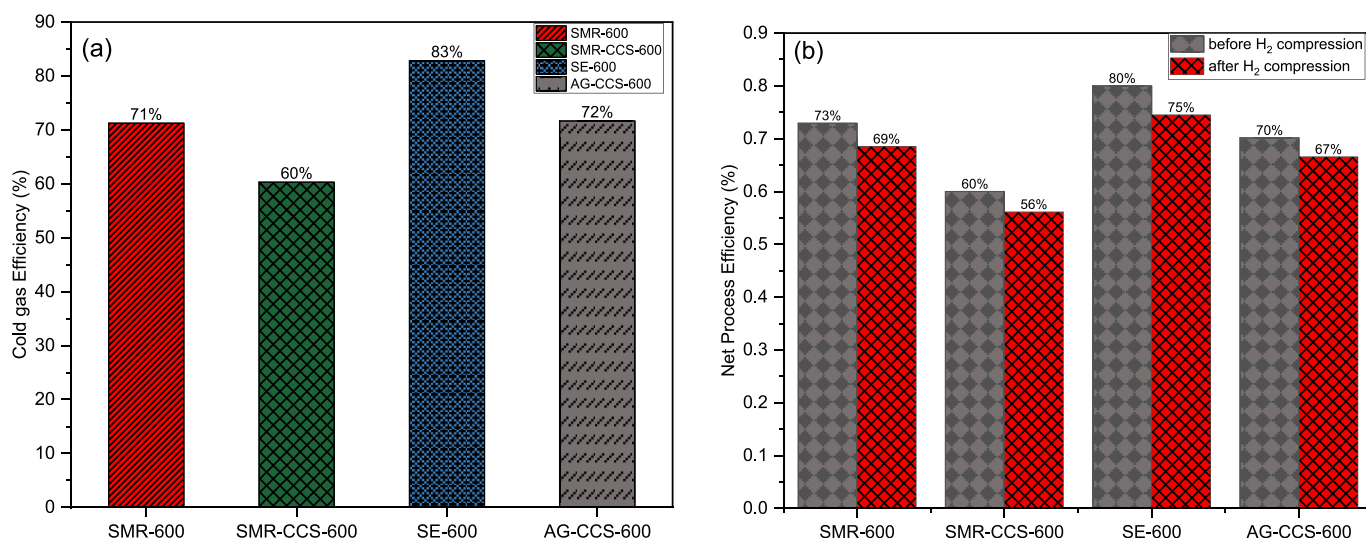


Fig. 9. (a) Cold gas efficiencies and (b) Net process efficiencies of the hydrogen production plants.

compression baselines.

Furthermore, this difference in net efficiency between these technologies stems partly from their distinct NG conversions. AG-CCS-600 achieved the highest fuel (NG) conversion of all the cases. The high fuel conversion results from the two-step reforming configuration in which 30 % conversion was seen in the GHR, while ATR completely converts the NG to ca. 99.2 %. It is important to acknowledge that in practice, achieving such high methane conversion could be challenging due to factors such as catalyst deactivation and heat and mass transfer limitations, which was not considered in this study. Fuel conversion from SE-600 reformer was observed to be lower than the AG-CCS-600 but higher than their counterpart SMR plants at 81.68 %.

3.4. Carbon capture efficiency and on-site CO₂ emissions

Table 7 shows the carbon capture efficiency and on-site CO₂ emissions intensities for the different hydrogen production facilities. Methane conversion in the SE-SR unit fell below 82 %, leaving some unconverted methane in the PSA off-gas, which can impact on the overall carbon capture efficiency in the plant. One drawback of SE-SR technology is the negative effects that higher operating pressures have on methane conversion and carbon capture efficiency, despite its in-situ CO₂ capture characteristics.

As the operating pressure increases, it influences the equilibrium of the endothermic reforming reaction in a way that makes it more difficult to fully convert the methane feedstock. With lower rates of reforming, more unreacted methane pass through to downstream units rather than being transformed into CO₂ and H₂. This low conversion reduces the amount of CO₂ available for capture, thereby weakening the process'

Table 7
Carbon capture performance of the examined hydrogen production technologies.

	Units	SMR-600	SMR-CCS-600	SE-600	ATR-600
Overall Carbon Capture efficiency	%	–	85.2	98.99	94.54
Specific CO ₂ Emissions	kg/kg H ₂	9.86	2.44	0.08	0.53
CO ₂ captured annually	kt/yr	–	1,634.03	1,274.41	1,463.34
CO ₂ emissions annually	kt/yr	1,555.31	385.68	12.95	84.245

overall carbon capture efficiency. A study by Abbas et al. [22] found that increasing the operating pressure of SE-SR of methane from 20 to 35 bar resulted in methane conversion dropping from 73.5 % to 64.8 % and CO₂ capture decreasing from 64.5 % to 58.8 %. Design modifications could help address such deterioration [29], but could drive up capital and operating costs. In our design, the lower methane conversion in the SE-SR unit is offset by the integrated oxy-fuel combustion unit. Since the oxy-fuel combustion uses pure oxygen (99 % purity) to burn the extra fuel and PSA off-gas stream, highly concentrated CO₂ stream is generated, leading to an improved overall carbon capture efficiency for the entire plant. Thus, CO₂ emissions from SE-600 plant was significantly reduced.

For SMR-CCS-600, the high natural gas consumption generated large volume of CO₂, which impacted on the overall carbon capture efficiency. AG-CCS-600 sits between the two with an overall carbon capture efficiency of about 94.5 %, in line with the findings of Cotton [80].

Inefficiencies in the CO₂ capture process can result in residual CO₂ emissions. Among the simulated blue hydrogen production plants, SE-600 had the lowest on-site CO₂ emissions at 0.08 kg CO₂/kg H₂, due to its high carbon capture efficiency. SMR-CCS-600 resulted in CO₂ emissions of 0.95 kg CO₂/kg H₂ owing to its relatively low carbon capture rate, while AG-CCS-600 maintained an intermediate emissions level of 0.53 kg CO₂/kg H₂. In comparison, SMR-600 yielded the highest emissions of all the hydrogen plants at 9.86 kg CO₂/kg H₂ as it lacks carbon capture step.

3.5. Economic performance

This section evaluates the relative economic competitiveness of each technology by examining the capital and operating costs associated with each production pathway. It also examines how the resulting production costs are influenced by hydrogen compression and carbon prices. Given the large capital investments required for carbon capture infrastructure, the levelised cost of hydrogen (LCOH) production and cost of CO₂ avoided (CCA) are important metrics for assessing the long-term economic competitiveness of blue hydrogen technologies. Therefore, this analysis focused on comparing these two indicators, alongside capital costs and operational costs. Table 8 presents a summary of the cost breakdown for all the hydrogen plants. 40 % contingency was added to SE-600 cost estimates to account for uncertainties associated with low TRL technologies, while 20 % was used for the other technologies.

The total plant cost for each of the technologies account for at least 60 % of the total capital investment, with AG-CCS-600 requiring the largest capital investment. The breakdown of the plant cost by

Table 8
Cost breakdown including capital and operating costs for all the cases studied.

(M£)	SMR-600	SMR-CCS-600	SE-600	ATR-600
Steam reformer and components	118.91	118.91	–	–
Fluidised bed reformer with Calciner and solid handling	–	–	107.76	–
PSA	–	–	63.88	33.55
H ₂ Compressor	34.27	34.27	50.74	23.44
Combustor	–	–	29.56	–
ATR	–	–	–	238.82
GHR	–	–	–	14.88
CCS Unit	–	158.88	–	98.44
Steam turbine	19.81	26.28	11.80	18.92
ASU and oxygen compressor	–	–	77.14	108.31
Shift converter	–	–	–	10.18
Auxiliary components and CO ₂ compressor	76.59	114.77	107.54	118.74
Total plant cost (TPC)	249.57	453.10	448.41	665.27
Contingency	49.91	90.62	179.37	133.05
Owner's costs	17.47	31.72	31.39	46.57
Spare parts cost	1.25	2.27	2.24	3.33
Working capital	28.40	33.56	24.66	28.30
Start-up costs	13.97	20.54	18.15	24.71
Total capital requirement (TCR)	360.58	631.80	704.22	901.24
Fixed costs				
Direct labour cost	1.38	1.50	1.50	1.49
Annual operating and maintenance cost	5.24	9.52	9.42	13.97
Administrative and general overhead cost	0.86	1.27	1.26	1.64
Indicative costs	6.24	11.33	11.21	16.63
Insurance	1.25	2.27	2.24	3.33
Local taxes and fees	1.25	2.27	2.24	3.33
Variable costs (M£)				
Fuel (Natural gas)	338.72	400.32	291.50	337.51
Water (Feed and Make up)	1.39	1.55	3.69	0.94
Catalysts	0.54	0.54	0.49	1.00
Other chemicals	0.10	0.10	0.10	0.10
MDEA	–	0.07	–	0.03
Piperazine	–	0.14	–	0.07
CaO	–	–	0.15	–
Electricity (with H ₂ compression)	18.61	40.9	44.68	37.09
CO ₂ transport & storage cost	0.00	16.34	12.75	14.63
Total OPEX (M£)	375.59	471.76	381.32	431.76
LCOH at zero carbon price (£/kg H ₂)	2.60	3.48	2.84	3.22
CCA at zero carbon price (£/ton CO ₂)	–	118.42	25.10	66.55
LCOH at carbon price of £83 (£/kg H ₂)	3.42	3.68	2.85	3.26
CCA at carbon price of £83 (£/ton CO ₂)	–	35.43	–57.89	–16.75

components for the hydrogen production technologies examined is displayed in Fig. 10.

The ATR equipment has the biggest share of the plant cost at approximately 36 %, in AG-CCS-600. It plays a key role in the generation of syngas and improving the overall fuel conversion of the process. Following closely is the ASU unit, which represents 16 % of the total plant cost. The CCS unit accounts for 15 % of the total plant cost, while the remaining 33 % is divided among the hydrogen compressor, GHR, and auxiliary components. For SE-600, the SE-SR equipment has the largest cost contribution, accounting for approximately 24 % of the total plant cost. This is followed by the ASU unit, which constitutes around 17 % of the total plant cost, while H₂ compressors and oxy-fuel combustion unit make up 11.32 % and 7.56 % of the total plant cost, respectively. The a-MDEA CCS unit is the primary cost driver in the SMR-CCS-600, accounting for roughly 35 % of the total plant cost. Additionally, the CO₂ compression unit accounts for 8 % of the total plant cost, which exceeds the 7.6 % contributed by the hydrogen compression unit. The large volume of flue gas generated due to the plant's high natural gas requirements directly impacts the size and, inevitably, the cost of the

CO₂ process equipment. Hydrogen compressors for SMR-600, SMR-CCS-600, SE-600 and AG-CCS-600 make up 13.73 %, 7.56 %, 11.32 % and 3.52 % of the total plant cost, respectively.

Moving beyond plant cost and total capital requirement, it is also important to consider the operating cost of the plant. These costs encompass labour, maintenance, energy consumption, and raw material expenditures. The running cost for SMR-600 plant exceeds its initial capital investments by 8.4 %, with natural gas accounting for more than 80 % of the operating cost. For SMR-CCS-600, the total OPEX is about 75 % of its TCR per annum. This means that for every £1 invested, the SMR-CCS plant will require £0.75 to operate a 600 MW hydrogen plant each year. Total OPEX for SE-600 is 53 % of its TCR, while ATR-600 will require 44 % of its initial capital investment to operate annually. Although some economic studies on conventional SMR have reported lower operating cost to capital costs ratio [81–83], the significant spike in the price of natural gas in the UK contributed to this increase in total OPEX reported in this study, as natural gas price has consistently increased by over 120 % between 2020 and January 2023 [64]. When fuel costs is excluded, the variable operating costs including electricity and water consumption, contributed most significantly to SE-600 operating costs. SE-600 has the highest estimated non-fuel variable costs among the technologies.

The LCOH was estimated for each hydrogen technology pathway based on their resulting capital and operating costs over a 25-year lifetime. At zero carbon price, SMR-600 had the lowest LCOH of £2.60/kg H₂, since carbon capture was not considered. Among the blue hydrogen technologies, SE-600 was found to have the lowest levelised cost of £2.84/kg H₂. This can be attributed to SE-SR's simpler design with fewer processing units, lowering both capital and operating expenses compared to the other technologies. AG-CCS-600 resulted in an intermediate levelised cost of £3.22/kg H₂ due to its high capital cost, while SMR-CCS-600 had the highest levelised cost at £3.48/kg H₂. It is challenging to directly compare the LCOH estimated in this study against literature values, due to natural variations in the modelling, plant configuration and capacity, costing methodologies and underlying assumptions applied such as carbon pricing, discount rates and natural gas prices.

However, the general trend of SE-600 and AG-CCS-600 having lower costs than SMR-CCS-600 aligns with previously reported trends for autothermal and SE-SR processes in literature [26,84,85]. For a ~ 60 MWth SE-SMR capacity, the findings of Dat Vo et al. [84] revealed that the SE-SMR system achieved an energy efficiency of 82.2 % based on lower heating value calculations. Moreover, they estimated SE-SMR production cost of £1.59/kgH₂ (after adjusting for inflation and currency conversion), representing a 12 % reduction in production cost compared to the conventional SMR with CCS alternative. Similarly, Diglio et al. reported a hydrogen production cost of £1.8/kgH₂ for an SE-SMR system integrated with fuel cell, which was lower than SMR with MEA CO₂ capture system by ~ 33 %. For a 1000 MWth autothermal and gas-heated reforming with CCS plant, Argyris et al. [14] reported LCOH range of £1.85 – £1.88/ kgH₂, lower than its counterpart SMR with CCS plant. The minor discrepancies in the numerical LCOH estimates between our analysis and other sources do not necessarily indicate disagreement, as our analysis incorporated hydrogen compression costs and a different carbon pricing.

Fig. 11 shows the breakdown of the levelised cost of hydrogen (LCOH) for the four different technologies based on capital costs, fuel costs, fixed and variable operating expenses (OPEX), and costs associated with CO₂ transport and storage via offshore. Total capital costs are the largest component of the LCOH for the SE-SR and ATR-GHR technologies except for the SMR and SMR-CCS-cases, where fuel cost make up the largest share of their LCOH. This is closely followed by the fuel cost for the SE-SR and ATR-GHR, capital costs for the SMR and SMR-CCS-cases, then the variable and the fixed O&M for all the cases. The CO₂ transport and storage costs are the smallest component of the LCOH for the blue hydrogen technologies. However, these costs are larger for

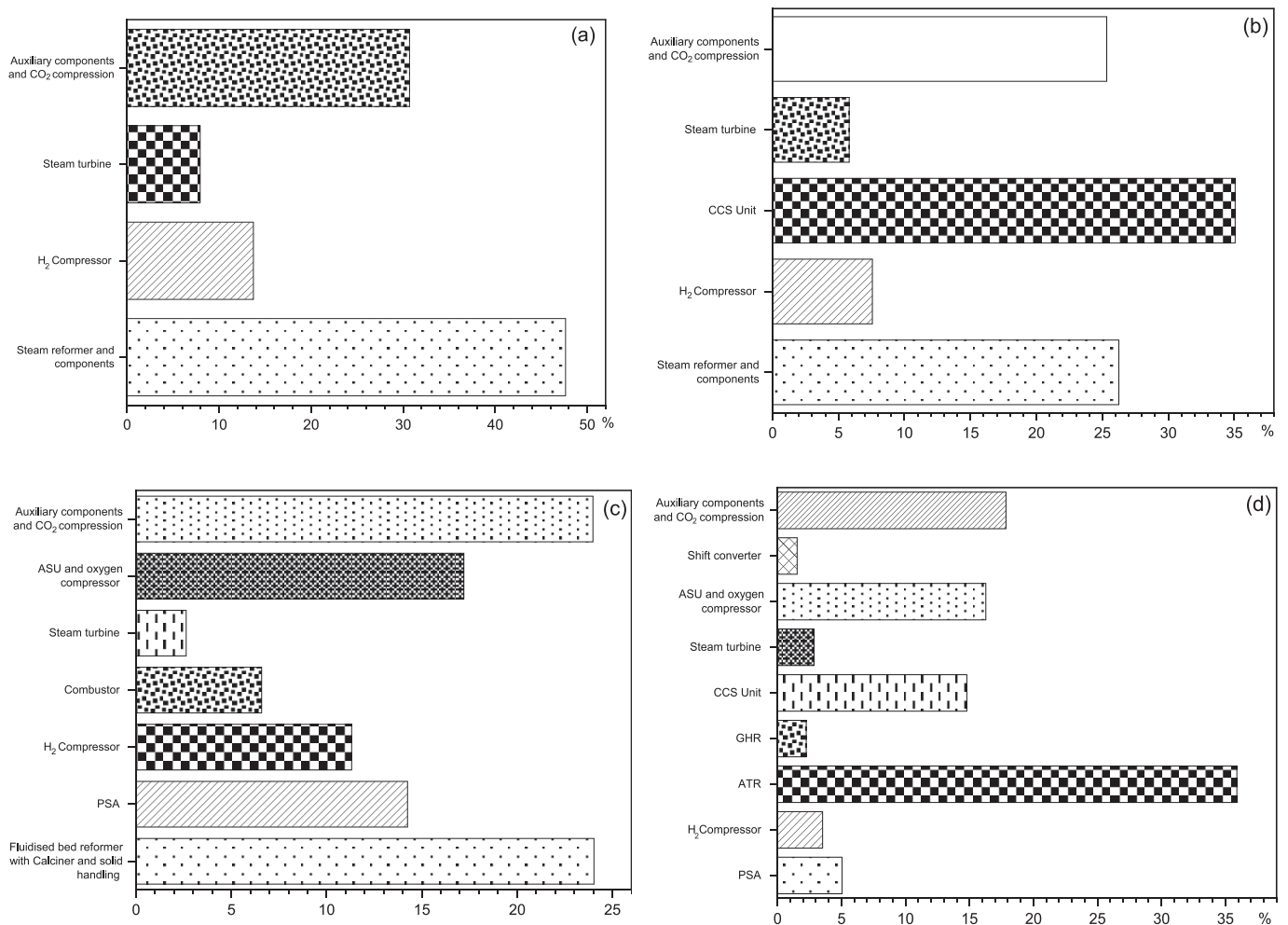


Fig. 10. Percentage distribution of total plant cost across (a) SMR-600, (b) SMR-CCS-600 (c) SE-600 and (d) AG-CCS-600.

the AG-CSS-600 and SMR-CCS-600 compared to SE-600, due to the volume of natural gas processed in these plants.

The cost of avoided CO₂ (CCA) emissions is also an important economic metric when evaluating low-carbon technologies. It is important to note that the method used in this study to calculate CCA depends on the extent of CO₂ reduction and the change in LCOH between the reference SMR plant (without CCS) and the blue hydrogen plant (see equation (9)). Simbeck and Beecy [86] highlighted three scenarios, using coal power plant as reference, to show how the CO₂ avoidance cost fluctuates depending on the reference and CCS plant. In this case, when there are small incremental increases in LCOH and significant reduction in CO₂ emissions, the CCA is low, whereas CCA is high when there are large increases in LCOH with small CO₂ reduction. In this study, the specific CO₂ emissions for SE-600 is 0.08 kg/kgH₂, which is a significant reduction from 9.64 kg/kgH₂ seen in the SMR-CCS-600. There was also a slight increase in LCOH from 2.60 £/kgH₂ (observed in the SMR) plant to 2.84 £/kgH₂ for SE-600, at zero carbon price. This results in lower CCA, when compared with AG-CCS-600 (specific CO₂ emission of 0.53 kg/kgH₂) and SMR-CCS-600 (specific CO₂ emission of 2.44 kg/kgH₂). The high CCA observed in SMR-CCS-600 is attributed to factors such as, high fuel consumption and cost and low net process efficiency. At zero carbon price, the cost of CO₂ avoided for the blue hydrogen technologies was estimated at £25.10–£118.42/tonne CO₂. SE-600 has the lowest avoidance cost of £25.10/tonne CO₂ due to its low hydrogen production costs. AG-CCS-600 had a CCA of £66.55/tonne CO₂, while SMR-CCS-600 had the highest CCA of £118.42/tonne CO₂.

As carbon price increases, the annual operating cost for the reference

SMR plant also increases due to the rising cost of CO₂ emissions. Consequently, this leads to a higher LCOH for the reference plant and low LCOH for the blue hydrogen plants. This change in LCOH, in turn, affects the calculated CCA for the blue hydrogen plants. The influence of carbon price on these costs will be elaborated upon in the remainder of this paper.

3.6. Impact of blue hydrogen production scale on cost

This section evaluates how the costs of SE-SR, ATR-GHR and SMR with carbon capture may be impacted at larger production scales more relevant for emerging commercial markets. Hydrogen production scale was increased from 600 MW to 1000 MWth (LHV). As production scale increased from 600 to 1000 MW, the capital requirement went up across all the examined technologies (see Fig. 12). Capital costs surged by a minimum of 30 % for each facility. SE-SR plant had the highest rise at 56 % but remained lower than the ATR-GHR plants, which have the highest TCR amongst the hydrogen technologies studied.

Fig. 13a shows that the LCOH for all the hydrogen plants decreases as the production scale increases from 600 to 1000 MW. This is primarily due to economies of scale, where the larger plants benefit from cost efficiencies and higher production volumes, resulting in lower costs per unit of hydrogen produced. At zero carbon price scenario, the calculated LCOH for the SE-600 plant is £2.84/kg, which reduces to £2.79/kg at 1000 MWth(LHV). This is a decrease of ~ 2 %. When the current average carbon price of 83 £/ton CO₂ is considered, similar reduction is observed. The LCOH of the AG-CCS-600 decreased by ~ 5.5 % from 3.22

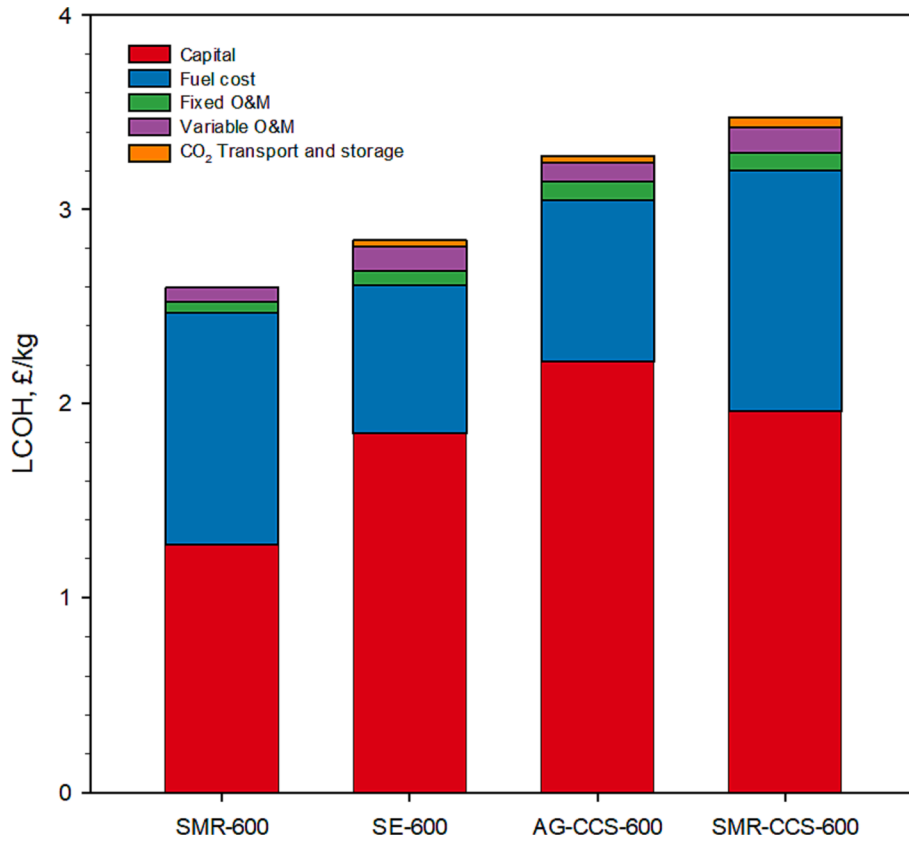


Fig. 11. Distribution of levelised cost of hydrogen (LCOH) for all the technologies studied at 600 MW_{th(LHV)} hydrogen production scale.

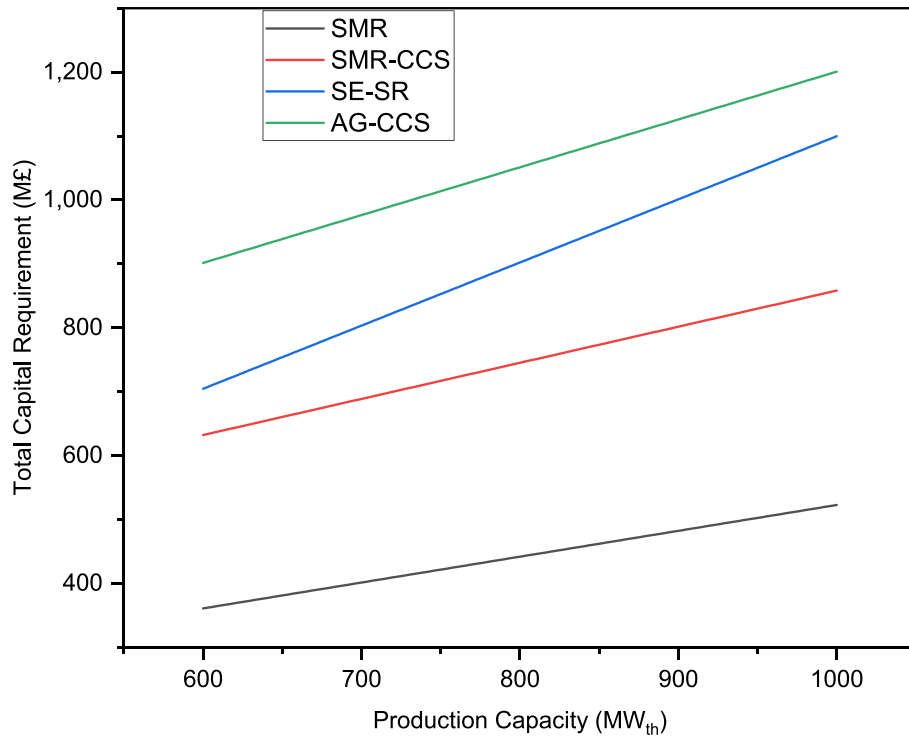


Fig. 12. (a) Total capital requirement of the various technologies when upscaled, and (b) the distribution of LCOH at 1000 MW_{th} hydrogen production capacity.

to 3.10 £/kgH₂, as the production scale increased to 1000 MW_{th(LHV)}. The SMR-CCS-case, which has the largest LCOH of the blue hydrogen plants, has its LCOH decrease by ~ 2.6 %, as the hydrogen production

scale increases from 600 to 1000 MW_{th(LHV)}.

The CCA also exhibits a similar pattern as hydrogen production scales up. For the SE-600 case, the CCA fell by 11.55 %, from 25.10 to

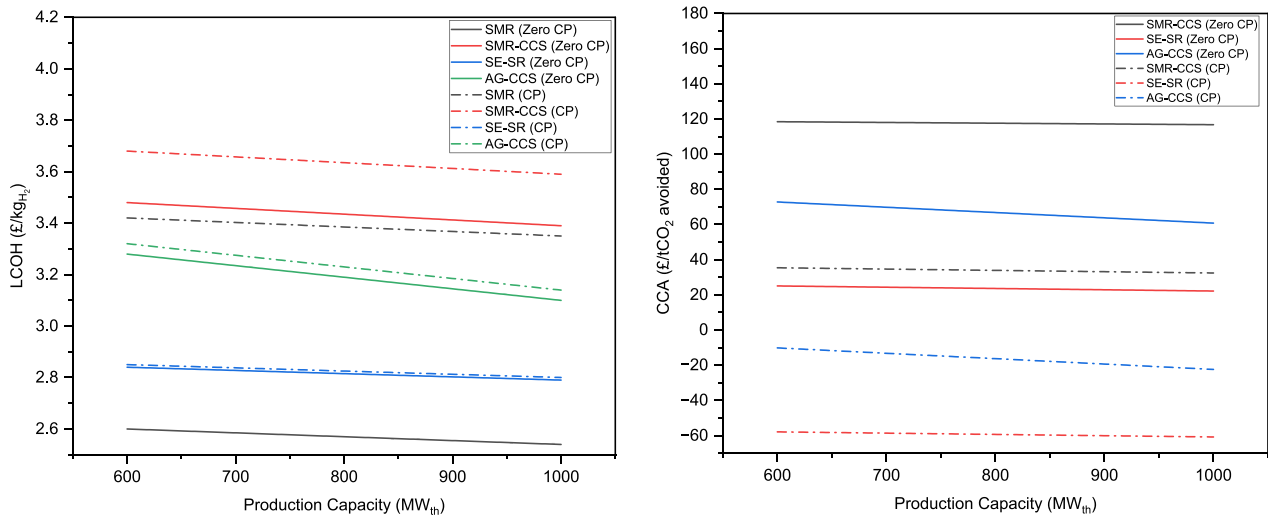


Fig. 13. (a) LCOH and (b) CCA of the various upscaled technologies at zero carbon price (CP) and carbon price - £83/tCO₂.

22.20 £/ton CO₂, when no carbon price considered. Similar reductions were observed in the AG-CCS and SMR-CCS cases, with CCA decreasing by 8 % (from 66.55 to 60.83 £/ton CO₂) and 1.42 % (from 118.42 to

116.74 £/ton CO₂) respectively, at zero carbon price. With the introduction of a carbon price, there was still an overall reduction in the CCA for the blue hydrogen technologies.

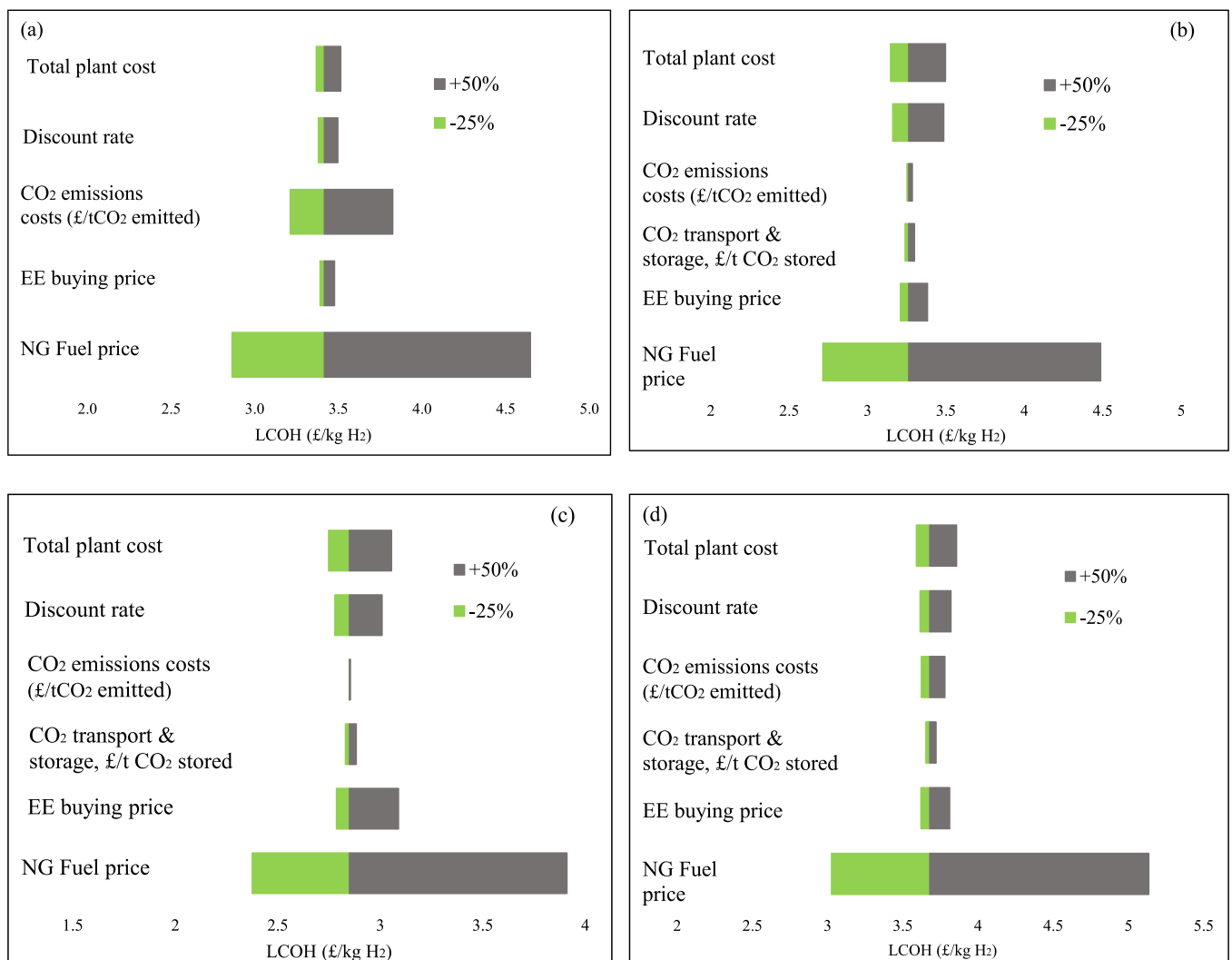


Fig. 14. Sensitivity of select variables on LCOH for (a) SMR (b) AG-CCS-600 (c) SE-600 and (d) SMR-CCS-600.

3.7. Sensitivity analysis

Sensitivity analysis was conducted to evaluate the impact of select input variables on the LCOH and CCA for the hydrogen technologies. The analysis varied total plant costs, natural gas prices, electricity prices, CO₂ transport and storage costs via offshore, CO₂ emissions costs, discount rates, and plant lifetime by -25 %/+50 % from the baseline values used in the primary economic assessment with a carbon price of 83 £/tCO₂. This wide input range was selected to capture potential changes and uncertainties in cost assumptions.

3.7.1. Natural gas price

As seen in Fig. 14, variations in natural gas price has the highest impact on the LCOH across all cases. For AG-CCS-600, the LCOH reduced to 2.71 £/kgH₂ at the lower sensitivity bound, and increased to around 4.48 £/kgH₂ at the upper sensitivity bound. Similarly, the LCOH for SE-600 ranged from approximately 2.37 to 3.9 £/kgH₂ for the upper and lower sensitivity bounds, respectively. The LCOH values for SMR-CCS-600 were 3.03 and 5.13 £/kgH₂ for the upper and lower sensitivity bounds, respectively.

CCA for SMR-CCS-600 is most affected by changes in natural gas prices. As natural gas prices rise, the CCA for SMR-CCS-600 reaches as high as 65.65£/tCO₂. This is due to the relatively large volume of natural

gas utilised in the SMR-CCS plants, invariably causing large increases in their LCOH. On the other hand, changes in CCA for SE-600 and AG-CCS-600 plants were relatively minimal with changes in natural gas price. The CCA for SE-600 ranged from (-5.0)£/tCO₂ to (-75.45) £/tCO₂ while that of AG-CCS-600 ranged from (-16.08) £/tCO₂ to (-17.30) £/tCO₂.

3.7.2. Electricity price

Among the various plants, SE-600 was the most affected by an increase in electricity prices, leading to an 8 % increase in the LCOH, relative to the reference value of 2.85£/kgH₂. This plant relies significantly on electricity imports, making it particularly sensitive to changes in electricity prices. In contrast, the LCOH of AG-CCS-600 and SMR-CCS-600 increased by 3.68 % and 3.60 %, respectively, with increase in electricity prices. The CCA for the plants are also seen to change slightly with variation in electricity prices.

3.7.3. CO₂ transport & storage

Our study considered offshore scenario for CO₂ transport and storage, considering the geographical location of the plants. The strategic location of the Humber region offers potential for supporting offshore CO₂ storage, and there are roadmaps already in place to make this a reality [87]. As seen in Fig. 14, the LCOH of SMR-CCS-600, AG-CCS-600 and SE-600 showed no significant increase, only dropping by ~ 0.7 %

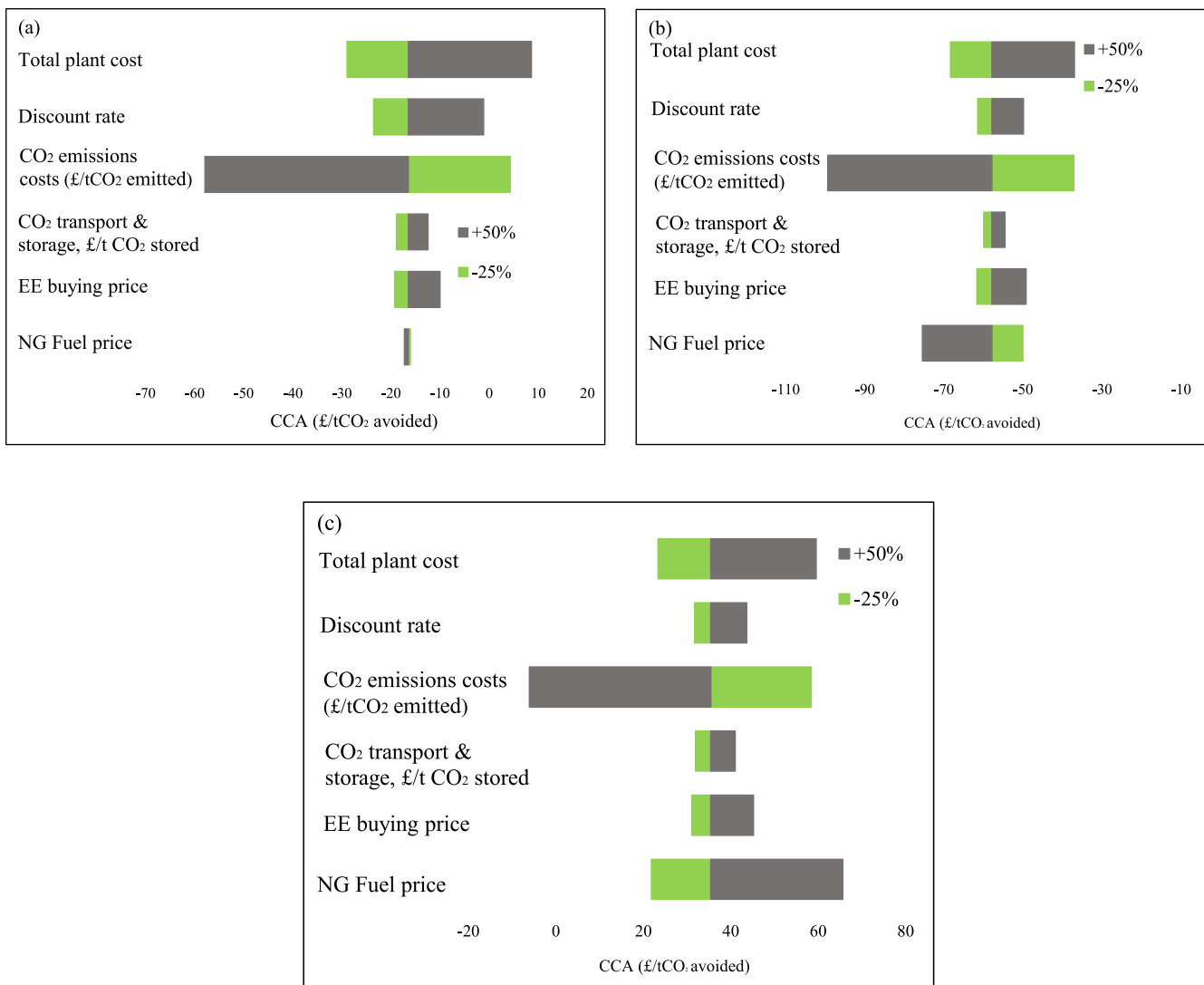


Fig. 15. Sensitivity of select variables on CCA for (a) AG-CCS-600 (b) SE-600 and (c) SMR-CCS-600.

and increasing $\sim 1\%$ at the lower and upper bounds, respectively. The cost of CO_2 transport and storage also had a slight impact on the CCA for these plants, ranging from 3% to 15% changes in CCA.

3.7.4. Carbon price

The monetary cost of CO_2 emissions was estimated from the carbon prices per tonne of CO_2 equivalent, based on the UK Emissions Trading Scheme. Fig. 14 shows that carbon price affects SMR-600 the most, after natural gas price, with its LCOH changing by 5% to 12% with variation in carbon price. The LCOH of SE-600 and AG-CCS-600 both fluctuate between 0.06% and 0.6% over the carbon price range. The LCOH of SMR-CCS-600 was observed to change much higher (2% and 3% at the upper and lower ranges, respectively) due to relatively large CO_2 emissions from the plant.

Fig. 15 revealed that among the input variables tested, carbon price had the strongest impact on the estimated CCA for the various blue hydrogen production facilities. A +50% change in the carbon price resulted in the largest swings in the CCA for each technology, with the CCA of SMR-CCS-600, SE-600 and AG-CCS-600 reducing by 117%, 71.6% and 250% relative to the base CCA, respectively. Reducing carbon price by 25% resulted in 64.9%, 35.8% and 126% increase in the CCA of SMR-CCS-600, SE-600 and AG-CCS-600, respectively. The relatively high change in the CCA of AG-CCS-600 shows that this technology is the most impacted by carbon price. This is likely due to the distinct relationship between natural gas consumption, CO_2 emissions and carbon capture efficiency, where huge volume of the relatively large CO_2 generated was captured. So, a price on each tonne of CO_2 avoided translates into a disproportionately large CCA.

To understand how carbon price can affect the economic competitiveness of these blue hydrogen technologies in the net-zero scenario, the carbon price sensitivity range was extended to consider the net-zero scenario (2050), which projects a central price of $\text{£}200/\text{tCO}_2\text{e}$ with a potential to rise to $\text{£}300/\text{tCO}_2\text{e}$ [88]. As seen in Fig. 16, the LCOH of the blue hydrogen technologies slightly increases with increasing carbon price while their CCA reduces with increasing carbon price. The negative values of CCA indicate cost savings associated with the use of these technologies. In this scenario, the use of these blue hydrogen technologies becomes desirable as the cost of avoiding CO_2 emissions is effectively offset and outweighed by benefits, such as the trading of carbon credits in carbon markets to provide additional revenue streams. For SMR-600, there was a sharp increase in its LCOH as carbon price increases. The LCOH of SMR-600 can reach high values of $\text{£}4.57/\text{kgH}_2$, when carbon price is at $200 \text{ £}/\text{ton CO}_2$. At a carbon price of $\sim \text{£}40/\text{ton CO}_2$ and $\text{£}70/\text{ton CO}_2$, the LCOH of SMR-600 increases to become equal to the LCOH of SE-600 and AG-CCS-600, respectively.

To compensate for the relatively high LCOH for SMR-CCS-600, the emissions cost must be much higher at $117 \text{ £}/\text{tCO}_2$ to justify the use of

SMR-CCS-600. At $117 \text{ £}/\text{tCO}_2$, the LCOH of SMR-CCS-600 becomes equal to SMR-600 and CCA turns negative, signifying cost savings from the use of CCS. However, following the UK's guidance on CCS achieving design capture rate of at least 95%, SMR-CCS-600 will need to demonstrate the achieved carbon capture efficiency [89]. At carbon prices above $\text{£}40\text{--}\text{£}117/\text{tCO}_2$, producing hydrogen without CCS (SMR-600) becomes more expensive than blue hydrogen, depending on the blue hydrogen technology.

In the net-zero scenario, the LCOH of SE-600, AG-CCS-600 and SMR-CCS-600 plants show a slight increase to 2.89, 3.27 and $3.96 \text{ £}/\text{kgH}_2$, respectively compared to 2.84, 3.22 and $3.48 \text{ £}/\text{kgH}_2$ at zero carbon price. This represents a 1.55%, 1.76% and 13.7% increase for SE-600, ATR-600 and SMR-CCS-600, respectively, which is insignificant compared to changes in their CCA. At a carbon price of $200 \text{ £}/\text{ton CO}_2$, the CCA of the blue hydrogen technologies are all negative at $-81.57 \text{ £}/\text{tCO}_2$, $-134.46 \text{ £}/\text{tCO}_2$ and $-174.88 \text{ £}/\text{tCO}_2$ avoided for SMR-CCS-600, AG-CCS-600 and SE-600, indicating potential revenues.

3.7.5. Discount rate

As seen in Fig. 14, the choice of discount rate has a noticeable impact on the LCOH of hydrogen. An upward trend in the LCOH was observed for all the plants as discount rate increases, with the SMR-CCS-600 plant displaying the highest value of $\text{£}3.81/\text{kgH}_2$ at 12% discount rate. Similarly, the cost of CO_2 avoidance followed a similar pattern, increasing as the discount rate increased.

3.7.6. Total plant cost

Fig. 14 revealed that the different low-carbon hydrogen production technologies exhibited varying degrees of susceptibility to increases or decreases in projected total plant cost. Of the three blue hydrogen technologies evaluated, SMR-CCS-600 demonstrated the lowest sensitivity to total plant cost. A +50% change in plant costs resulted in about 4.8% increase in LCOH for SMR-CCS-600, whereas $\sim 7.1\%$ increase in LCOH was observed for both AG-CCS-600 and SE-600 plants. Reducing plant cost by 25% resulted in 2.4% drop in the LCOH of SMR-CCS-600 and $\sim 3.6\%$ decrease in the LCOH of AG-CCS-600 and SE-600 plants.

When assessing the impact of total plant cost on CCA, the CCA estimate for AG-CCS showed the greatest sensitivity, reducing by 76% when plant cost is lowered by 25% and increasing by 152% at +50% plant cost range. SMR-CCS-600 showed intermediate sensitivity on CCA, fluctuating by roughly 34% and 68% at the lower and upper sensitivity bounds, respectively. Meanwhile, SE displayed the lowest sensitivity amongst the technologies, with its CCA changing by 18% and 36% at the lower and upper sensitivity bounds, respectively. Total plant cost has the second-greatest impact on the CCA of SE-600 and AG-CCS-600, after carbon price, and third-greatest impact on the CCA of SMR-CCS-600, after carbon price and natural gas price.

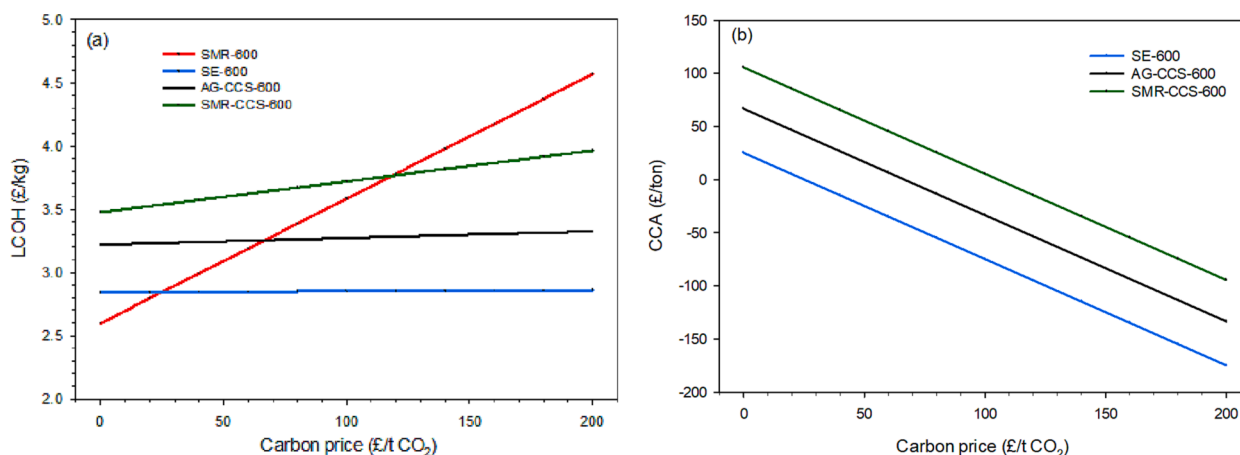


Fig. 16. Sensitivity of (a) LCOH and (b) CCA to changes in carbon prices.

4. Conclusion

In this study, the potential of scaling up the emerging SE-SR technology was evaluated through a techno-economic assessment. With the goal of benchmarking the SE-SR technology, it was compared against SMR-CCS, ATR-GHR-aMDEA, and a base case conventional SMR at large-scale blue hydrogen production, 600 MW_{th(LHV)} and scaled up to 1000 MW_{th(LHV)}. Sensitivity of natural gas price, electricity price, CO₂ transport and storage cost, carbon price, total plant cost and discount rate on two key indicators: LCOH and CCA was also conducted for all the cases examined.

The SMR-CCS plant has the lowest technical performance of all the cases considered in this study. The net process efficiency dropped from ~ 69 % to ~ 56 %, when CCS unit was integrated into the process. In addition, its overall carbon capture efficiency was below 90 %. Whilst AG-CCS-600 exhibited the highest high fuel conversion of ~ 99 %, its net process efficiencies was low, reaching ca. 66 %. This is because of the energy intensive ASU, H₂ compressor and CCS plant, which will require electricity imports of, at least, 30 MWe to operate. Conversely, SE-600 plant had the highest net process efficiency of ~ 74 %, with the overall carbon capture efficiency reaching 98 %. The specific CO₂ emissions for SMR, SMR-CCS, SE-SR and ATR-GHR-aMDEA plants were found to be around 9.86, 2.44, 0.08 and 0.53 kgCO₂/kgH₂, respectively.

Upon scaling the plants from 600 to 1000 MW capacity, the LCOH and CCA reduced for all the technologies. At a carbon price of 83 £/tCO_{2e}, the LCOH of SMR-CCS-600 is the highest at 3.68£/kgH₂, mainly attributed to the large volume of natural gas required to operate the process. The SMR plant had relatively higher LCOH at 3.42 £/kgH₂, due to its high emissions costs which are a result of the significant volume of CO₂ generated and emitted from the plants. LCOH for AG-CCS-600 was at 3.26 £/kgH₂, with capital costs as the major cost contributor, primarily due to the high cost of components such as autothermal reformers and the a-MDEA CCS plants. For SE-600, the LCOH was estimated to be 2.85 £/kgH₂, due to its compact nature and low natural gas consumption. Factors such as natural gas prices, electricity prices, carbon price and total plant costs exerted notable impact on the LCOH and CCA for the hydrogen technologies. Natural gas price has the greatest impact on the LCOH for the technologies, while carbon price impacts the CCA mostly.

Whilst our assessment shows that SE-SR has promising technical and cost-effective potential for large-scale blue hydrogen production, it is also important to highlight drawbacks that can slow down its commercialisation. As discussed earlier concerning decreased methane conversion and carbon capture efficiency at higher operating pressures; more design configurations need to be explored at lower operating pressure conditions to determine if they can achieve equivalent or improved performance compared to higher pressure designs, while also assessing any economic impacts from changed compression requirements. Our design considered the use of PSA off-gas as fuel for oxy-combustion to provide heat for calcination, which could present control challenges due to the variable composition of this fuel stream. Thus, research efforts should pursue other heat integration solutions such as electrically-heated calcination or the use of renewable energy, while intensifying the SE-SR. In addition to its relatively low TRL, there are also challenges with maintaining sufficient sorbent capacity over multiple adsorption/desorption cycles due to sorbent degradation, which over time reduces carbon capture efficiency. Therefore, pilot testing is still needed to prove the durability of sorbents over long campaigns, and heat and mass transfer performance within higher pressure sorbent beds. The HyPER project led by Cranfield University, UK is already considering this option.

Declaration of competing interest

The authors declare that they have no known competing financial interests or personal relationships that could have appeared to influence

the work reported in this paper.

Data availability

Data will be made available on request.

Acknowledgment

The authors would like to acknowledge the funding provided by the Net Zero Research (formerly BF2RA) Grant 38 to undertake this research, and thank EDF Energy for their technical support.

Appendix A. Supplementary data

Supplementary data to this article can be found online at <https://doi.org/10.1016/j.enconman.2024.118132>.

References

- [1] HM Government The Ten Point Plan for a Green Industrial Revolution 2020.
- [2] HM Government Net Zero Strategy Build Back Greener 2021.
- [3] IEA. Global Hydrogen Review 2023. IEA 2023. <https://www.iea.org/reports/global-hydrogen-review-2023> (accessed November 29, 2023).
- [4] Chi J, Yu H. Water electrolysis based on renewable energy for hydrogen production. *Chin J Catal* 2018;39:390–4. [https://doi.org/10.1016/S1872-2067\(17\)62949-8](https://doi.org/10.1016/S1872-2067(17)62949-8).
- [5] Lagioia G, Spinielli MP, Amicarelli V. Blue and green hydrogen energy to meet European Union decarbonisation objectives. an overview of perspectives and the current state of affairs. *Int J Hydrogen Energy* 2023;48:1304–22. <https://doi.org/10.1016/j.ijhydene.2022.10.044>.
- [6] Pastore LM, Lo Basso G, Sforzini M, de Santoli L. Technical, economic and environmental issues related to electrolyzers capacity targets according to the Italian Hydrogen Strategy: a critical analysis. *Renew Sustain Energy Rev* 2022;166: 112685. <https://doi.org/10.1016/j.rser.2022.112685>.
- [7] Safari A, Das N, Langhelle O, Roy J, Assadi M. Natural gas: a transition fuel for sustainable energy system transformation? *Energy Sci Eng* 2019;7:1075–94. <https://doi.org/10.1002/ese3.380>.
- [8] Edwards RL, Font-Palma C, Howe J. The status of hydrogen technologies in the UK: a multi-disciplinary review. *Sustainable Energy Technol Assess* 2021;43:100901. <https://doi.org/10.1016/j.seta.2020.100901>.
- [9] Nikolaidis P, Poullikkas A. A comparative overview of hydrogen production processes. *Renew Sustain Energy Rev* 2017;67:597–611. <https://doi.org/10.1016/j.rser.2016.09.044>.
- [10] LeValley TL, Richard AR, Fan M. The progress in water gas shift and steam reforming hydrogen production technologies – a review. *Int J Hydrogen Energy* 2014;39:16983–7000. <https://doi.org/10.1016/j.ijhydene.2014.08.041>.
- [11] Lamb JJ, Hillestad M, Rytter E, Bock R, Nordgård ASR, Lien KM, et al. Traditional routes for hydrogen production and carbon conversion. *Hydrogen, Biomass and Bioenergy*, Elsevier 2020:21–53. <https://doi.org/10.1016/B978-0-08-102629-8.00003-7>.
- [12] Nnabuiife SG, Ugbeh-Johnson J, Okeke NE, Ogbonnaya C. Present and projected developments in hydrogen production: a technological review*. *Carbon Capture Science & Technology* 2022;3:100042. <https://doi.org/10.1016/j.ccs.2022.100042>.
- [13] Mahabir J, Samaroo N, Janardhanan M, Ward K. Pathways to sustainable methanol operations using gas-heated reforming (GHR) technologies. *J CO2 Util* 2022;66: 102302. <https://doi.org/10.1016/j.jcou.2022.102302>.
- [14] Argyris PA, Wong J, Wright A, Pereira LMC, Spallina V. Reducing the cost of low-carbon hydrogen production via emerging chemical looping process. *Energy Convers Manag* 2023;277:116581. <https://doi.org/10.1016/j.enconman.2022.116581>.
- [15] Luis P. Use of monoethanolamine (MEA) for CO₂ capture in a global scenario: consequences and alternatives. *Desalination* 2016;380:93–9. <https://doi.org/10.1016/j.desal.2015.08.004>.
- [16] Wang Y, Zhao L, Otto A, Robinius M, Stolten D. A review of post-combustion CO₂ capture technologies from coal-fired power plants. *Energy Procedia* 2017;114: 650–65. <https://doi.org/10.1016/j.egypro.2017.03.1209>.
- [17] Collidi G. Reference data and Supporting Literature Reviews for SMR Based Hydrogen Production with CCS. 2017.
- [18] Mudhasakul S, Ku H. PL.A simulation model of a CO₂ absorption process with methyldiethanolamine solvent and piperazine as an activator. *Int J Greenhouse Gas Control* 2013;15:134–41. <https://doi.org/10.1016/j.IJGGC.2013.01.023>.
- [19] Oh H-T, Kum J, Park J, Dat Vo N, Kang J-H, Lee C-H. Pre-combustion CO₂ capture using amine-based absorption process for blue H₂ production from steam methane reformer. *Energy Convers Manag* 2022;262:115632. <https://doi.org/10.1016/j.enconman.2022.115632>.
- [20] Kum J, Oh H-T, Park J, Kang J-H, Lee C-H. Techno-economic analysis and optimization of a CO₂ absorption process with a solvent looping system at the absorber using an MDEA/PZ blended solvent for steam methane reforming. *Chem Eng J* 2023;455:140685. <https://doi.org/10.1016/j.cej.2022.140685>.

- [21] Udemu C, Font-Palma C. Modelling of sorption-enhanced steam reforming (SE-SR) process in fluidized bed reactors for low-carbon hydrogen production: a review. *Fuel* 2023;340:127588. <https://doi.org/10.1016/j.fuel.2023.127588>.
- [22] Abbas SZ, Dupont V, Mahmud T. Modelling of H₂ production in a packed bed reactor via sorption enhanced steam methane reforming process. *Int J Hydrogen Energy* 2017;42:18910–21.
- [23] Cobden PD, Elzinga GD, Booneveld S, Dijkstra JW, Jansen D, van den Brink RW. Sorption-enhanced steam-methane reforming: CaO–CaCO₃ capture technology. *Energy Procedia* 2009;1:733–9. <https://doi.org/10.1016/J.EGYPRO.2009.01.097>.
- [24] Johnsen K, Ryu HJ, Grace JR, Lim CJ. Sorption-enhanced steam reforming of methane in a fluidized bed reactor with dolomite as CO₂-acceptor. *Chem Eng Sci* 2006;61:1195–202. <https://doi.org/10.1016/j.ces.2005.08.022>.
- [25] Ochoa-Fernández E, Haugen G, Zhao T, Rønning M, Aartun I, Borresen B, et al. Process design simulation of H₂ production by sorption enhanced steam methane reforming: evaluation of potential CO₂ acceptors. *Green Chem* 2007;9:654–66. <https://doi.org/10.1039/b614270b>.
- [26] Diglio G, Hanak DP, Bareschino P, Mancusi E, Pepe F, Montagnaro F, et al. Techno-economic analysis of sorption-enhanced steam methane reforming in a fixed bed reactor network integrated with fuel cell. *J Power Sources* 2017;364:41–51. <https://doi.org/10.1016/J.JPOWSOUR.2017.08.005>.
- [27] Yan Y, Manovic V, Anthony EJ, Clough PT. Techno-economic analysis of low-carbon hydrogen production by sorption enhanced steam methane reforming (SE-SMR) processes. *Energy Convers Manag* 2020;226:113530. <https://doi.org/10.1016/j.enconman.2020.113530>.
- [28] Meyer J, Mastin J, Bjørnebole TK, Ryberg T, Eldrup N. Techno-economic study of the Zero Emission Gas power concept. *Energy Procedia* 2011;4:1949–56. <https://doi.org/10.1016/J.EGYPRO.2011.02.075>.
- [29] Yan Y, Thanganadar D, Clough PT, Mukherjee S, Patchigolla K, Manovic V, et al. Process simulations of blue hydrogen production by upgraded sorption enhanced steam methane reforming (SE-SMR) processes. *Energy Convers Manag* 2020;222:113144. <https://doi.org/10.1016/j.enconman.2020.113144>.
- [30] H.W. Langmi N, Engelbrecht P.M, Modisha D, Bessarabov Hydrogen storage Electrochemical Power Sources: Fundamentals, Systems, and Applications, Elsevier 2022 455 486 10.1016/B978-0-12-819424-9.00006-9.
- [31] Sdanghi G, Maranzana G, Celzard A, Fierro V. Review of the current technologies and performances of hydrogen compression for stationary and automotive applications. *Renew Sustain Energy Rev* 2019;102:150–70. <https://doi.org/10.1016/j.rser.2018.11.028>.
- [32] Valente A, Iribarren D, Dufour J. Harmonised life-cycle global warming impact of renewable hydrogen. *J Clean Prod* 2017;149:762–72. <https://doi.org/10.1016/j.jclepro.2017.02.163>.
- [33] Equinor ASA. H₂H Saltend: The first step to a Zero Carbon Humber 2020.
- [34] Salem M, Shoaib AM, Ibrahim AFM. Simulation of a natural gas steam reforming plant for hydrogen production optimization. *Chem Eng Technol* 2021;44:1651–9. <https://doi.org/10.1002/CEAT.202100123>.
- [35] Galletti C, Specchia S, Saracco G, Specchia V. Gold-supported catalysts for medium temperature-water gas shift reaction. *Top Catal* 2009;52:688–92. <https://doi.org/10.1007/S11244-009-9213-5/FIGURES/5>.
- [36] Sircar S, Golden TC. Purification of hydrogen by pressure swing adsorption. *Sep Sci Technol* 2000;35:667–87. <https://doi.org/10.1081/SS-100100183>.
- [37] Fernandez JR, Abanades JC, Murillo R. Modeling of sorption enhanced steam methane reforming in an adiabatic fixed bed reactor. *Chem Eng Sci* 2012;84:1–11. <https://doi.org/10.1016/j.ces.2012.07.039>.
- [38] Arias B, Diego ME, Méndez A, Alonso M, Abanades JC. Calcium looping performance under extreme oxy-fuel combustion conditions in the calciner. *Fuel* 2018;222:711–7. <https://doi.org/10.1016/j.fuel.2018.02.163>.
- [39] Jayarathna CK, Mathisen A, Øi LE, Tokheim L-A. Aspen Plus® process simulation of calcium looping with different indirect calciner heat transfer concepts. *Energy Procedia* 2017;114:201–10. <https://doi.org/10.1016/j.egypro.2017.03.1162>.
- [40] French S. The role of zero and low carbon hydrogen in enabling the energy transition and the path to net zero greenhouse gas emissions. *Johnson Matthey Technol Rev* 2020;64:357–70. <https://doi.org/10.1595/205651320x15910225395383>.
- [41] Matthey J. LCHTM Process for the production of blue hydrogen. UK: Billingham; 2022.
- [42] Zhao B, Liu F, Cui Z, Liu C, Yue H, Tang S, et al. Enhancing the energetic efficiency of MDEA/PZ-based CO₂ capture technology for a 650 MW power plant: process improvement. *Appl Energy* 2017;185:362–75. <https://doi.org/10.1016/J.APENERGY.2016.11.009>.
- [43] Romano MC, Chiesa P, Lozza G. Pre-combustion CO₂ capture from natural gas power plants, with ATR and MDEA processes. *Int J Greenhouse Gas Control* 2010; 4:785–97. <https://doi.org/10.1016/J.IJGGC.2010.04.015>.
- [44] Mudhasakul S, Ku H, Douglas PL. A simulation model of a CO₂ absorption process with methyldiethanolamine solvent and piperazine as an activator. *Int J Greenhouse Gas Control* 2013;15:134–41. <https://doi.org/10.1016/j.ijggc.2013.01.023>.
- [45] Feyzi V, Beheshti M, Gharibi KA. Exergy analysis: A CO₂ removal plant using a-MDEA as the solvent. *Energy* 2017;118:77–84. <https://doi.org/10.1016/j.energy.2016.12.020>.
- [46] Aspen Technology Inc. Aspen Plus® 2022.
- [47] Bains M. Hill (nee Robinson) L, Rossington P. *Fuels: Natural gas*. Bristol; 2016.
- [48] Martínez I, Grasa G, Meyer J, Di Felice L, Kazi S, Sanz C, et al. Performance and operating limits of a sorbent-catalyst system for sorption-enhanced reforming (SER) in a fluidized bed reactor. *Chem Eng Sci* 2019;205:94–105. <https://doi.org/10.1016/J.CES.2019.04.029>.
- [49] Zhu L, Li L, Fan J. A modified process for overcoming the drawbacks of conventional steam methane reforming for hydrogen production: Thermodynamic investigation. *Chem Eng Res Des* 2015;104:792–806. <https://doi.org/10.1016/j.cherd.2015.10.022>.
- [50] Hong J, Field R, Gazzino M, Ghoniem AF. Operating pressure dependence of the pressurized oxy-fuel combustion power cycle. *Energy* 2010;35:5391–9. <https://doi.org/10.1016/j.energy.2010.07.016>.
- [51] Buhre BJP, Elliott LK, Sheng CD, Gupta RP, Wall TF. Oxy-fuel combustion technology for coal-fired power generation. *Prog Energy Combust Sci* 2005;31: 283–307. <https://doi.org/10.1016/j.pecs.2005.07.001>.
- [52] Garduner M. DOE Hydrogen and Fuel Cells Program Record 9013: Energy requirements for hydrogen gas compression and liquefaction as related to vehicle storage needs. 2009.
- [53] Al-Zareer M, Dincer I, Rosen MA. Analysis and assessment of a hydrogen production plant consisting of coal gasification, thermochemical water decomposition and hydrogen compression systems. *Energy Convers Manag* 2018; 157:600–18. <https://doi.org/10.1016/j.enconman.2017.11.047>.
- [54] C.W. White ASPEN plus simulation of CO₂ recovery process 2002 Pittsburgh, PA, and Morgantown, WV (United States) 10.2172/810497.
- [55] Patchigolla K, Oakey JE. Design overview of high pressure dense phase CO₂ pipeline transport in flow mode. *Energy Procedia* 2013;37:3123–30. <https://doi.org/10.1016/j.egypro.2013.06.198>.
- [56] Department for Business E& IS (BEIS). Digest of UK Energy Statistics (DUKES) 2022.
- [57] The International Energy Agency (IEA). *Toward a Common Method of Cost Estimation for CO₂ Capture and Storage at Fossil Fuel Power Plants*. 2013.
- [58] IEA Greenhouse Gas R&D Programme (IEA GHG). *Criteria for Technical and Economic Assessment of Plants with Low CO₂ Emissions*. 2009.
- [59] Peters MS, Timmerhaus KD, West RE. *Plant Design and Economics for Chemical Engineers*. 5th ed. McGraw-Hill Education; 2003.
- [60] Towler G, Sinnott R. *Chemical engineering design: principles, practice and economics of plant and process design*. Butterworth-Heinemann; 2021.
- [61] Department for Business E& IS (BEIS). *Hydrogen Production Costs 2021*. 2021.
- [62] Ofgem. *Electricity Prices: Forward Delivery Contracts - Weekly Average (GB)*. Office of Gas and Electricity Markets 2023. <https://www.ofgem.gov.uk/energy-data-and-research/data-portal/wholesale-market-indicators> (accessed April 7, 2023).
- [63] Department for Energy Security and Net Zero. *Prices of fuels purchased by manufacturing industry in Great Britain. Quarterly Energy Prices Publication 2023*. <https://www.gov.uk/government/statistical-data-sets/prices-of-fuels-purchased-by-manufacturing-industry> (accessed April 26, 2023).
- [64] Ofgem. *Gas Prices: Forward Delivery Contracts - Weekly Average (GB)*. Office of Gas and Electricity Markets 2023. <https://www.ofgem.gov.uk/energy-data-and-research/data-portal/wholesale-market-indicators> (accessed April 7, 2023).
- [65] Yorkshire Water. *Wholesale Charges Scheme Non-household 2023/2024*. 2023.
- [66] Reforming Catalyst Manufacturers 2023. <https://www.alibaba.com/products/steam-reforming-catalyst.html> (accessed April 9, 2023).
- [67] MDEA Price CAS 105-59-9 2023. <https://www.made-in-china.com/> (accessed April 9, 2023).
- [68] PharmaCompass. Piperazine | Price | Per kg | USD 2023. <https://www.pharmacompass.com/active-pharmaceutical-ingredients/piperazine> (accessed April 9, 2023).
- [69] IndexBox. *Chalk Dolomite Price in the UK - 2023 2023*. <https://www.indexbox.io/search/chalk-and-dolomite-price-the-uk/> (accessed March 7, 2023).
- [70] Pale Blue Dot Energy. *Progressing development of the UK's strategic carbon dioxide storage resource. A Summary of Results from the Strategic UK CO₂ 2016;2*.
- [71] Department for Business Energy & Industrial Strategy. *UK ETS: Carbon prices for use in civil penalties, 2023 2022*. <https://www.gov.uk/government/publications/determinations-of-the-uk-ets-carbon-price/uk-ets-carbon-prices-for-use-in-civil-penalties-2023#:~:text=the%20carbon%20price%20for%20the%20scheme%20year%20beginning,January%202023%20is%20%C2%A383.03> (accessed November 20, 2023).
- [72] Leroutier M. Carbon pricing and power sector decarbonization: evidence from the UK. *J Environ Econ Manage* 2022;111:102580. <https://doi.org/10.1016/j.jeem.2021.102580>.
- [73] Tsiklotos C, Hermsmann M, Müller TE. Hydrogen transport in large-scale transmission pipeline networks: thermodynamic and environmental assessment of repurposed and new pipeline configurations. *Appl Energy* 2022;327:120097. <https://doi.org/10.1016/j.apenergy.2022.120097>.
- [74] Briottet L, Batisse R, de Dinechin G, Langlois P, Thiers L. Recommendations on X80 steel for the design of hydrogen gas transmission pipelines. *Int J Hydrogen Energy* 2012;37:9423–30. <https://doi.org/10.1016/j.ijhydene.2012.02.009>.
- [75] Khan MA, Young C, Mackinnon C, Layzell D. *The techno-economics of hydrogen compression. Transition Accelerator Technical Briefs* 2021;1:1–36.
- [76] Liao L, Zheng J, Li C, Liu R, Zhang Y. Thermodynamic modeling modification and experimental validation of entrained-flow gasification of biomass. *J Energy Inst* 2022;103:160–8. <https://doi.org/10.1016/j.joei.2022.06.006>.
- [77] HajiHashemi M, Mazhkoo S, Dadfar H, Livani E, Naseri Varnosefaderani A, Pourali O, et al. Combined heat and power production in a pilot-scale biomass gasification system: experimental study and kinetic simulation using ASPEN Plus. *Energy* 2023;276:127506. <https://doi.org/10.1016/j.energy.2023.127506>.
- [78] Collodi G, Azzaro G, Ferrari N, Santos S. Techno-economic evaluation of deploying CCS in SMR based merchant H₂ production with NG as feedstock and fuel. *Energy Procedia* 2017;114:2690–712. <https://doi.org/10.1016/j.egypro.2017.03.1533>.
- [79] Abbas SZ, Dupont V, Mahmud T. Modelling of H₂ production via sorption enhanced steam methane reforming at reduced pressures for small scale

- applications. *Int J Hydrogen Energy* 2019;44:1505–13. <https://doi.org/10.1016/j.ijhydene.2018.11.169>.
- [80] Bill Cotton. Clean hydrogen: Hydrogen from natural gas through cost effective CO2 capture. 2021.
- [81] Alrashed F, Zahid U. Comparative analysis of conventional steam methane reforming and PdAu membrane reactor for the hydrogen production. *Comput Chem Eng* 2021;154:107497. <https://doi.org/10.1016/j.compchemeng.2021.107497>.
- [82] Oni AO, Anaya K, Giwa T, Di Lullo G, Kumar A. Comparative assessment of blue hydrogen from steam methane reforming, autothermal reforming, and natural gas decomposition technologies for natural gas-producing regions. *Energy Convers Manag* 2022;254:115245. <https://doi.org/10.1016/j.enconman.2022.115245>.
- [83] Keipi T, Tolvanen H, Konttinen J. Economic analysis of hydrogen production by methane thermal decomposition: comparison to competing technologies. *Energy Convers Manag* 2018;159:264–73. <https://doi.org/10.1016/j.enconman.2017.12.063>.
- [84] Dat Vo N, Kang JH, Oh M, Lee CH. Dynamic model and performance of an integrated sorption-enhanced steam methane reforming process with separators for the simultaneous blue H2 production and CO2 capture. *Chem Eng J* 2021;423:130044. <https://doi.org/10.1016/J.CEJ.2021.130044>.
- [85] Khojasteh Salkuyeh Y, Saville BA, MacLean HL. Techno-economic analysis and life cycle assessment of hydrogen production from natural gas using current and emerging technologies. *Int J Hydrogen Energy* 2017;42:18894–909. <https://doi.org/10.1016/j.ijhydene.2017.05.219>.
- [86] Simbeck D, Beecy D. The CCS paradox: the much higher CO2 avoidance costs of existing versus new fossil fuel power plants. *Energy Procedia* 2011;4:1917–24. <https://doi.org/10.1016/j.egypro.2011.02.071>.
- [87] Clery D, Gough C. Cluster mapping report. *The Humber Industrial Cluster 2022*.
- [88] Department for Business Energy & Industrial Strategy. Guidance on estimating carbon values beyond 2050: an interim approach. n.d.
- [89] Environment Agency. Post-combustion carbon dioxide capture: best available techniques (BAT). Guidance 2022. <https://www.gov.uk/guidance/post-combustion-carbon-dioxide-capture-best-available-techniques-bat> (accessed August 27, 2023).